



Contents lists available at ScienceDirect

## Bioorganic &amp; Medicinal Chemistry

journal homepage: [www.elsevier.com/locate/bmc](http://www.elsevier.com/locate/bmc)

## Structure-guided design and development of novel benzimidazole class of compounds targeting DNA gyraseB enzyme of *Staphylococcus aureus*

Renuka Janupally<sup>a</sup>, Variam Ullas Jeankumar<sup>a</sup>, Karyakulam Andrews Bobesh<sup>a</sup>, Vijay Soni<sup>a</sup>, Parthiban Brindha Devi<sup>a</sup>, Venkat Koushik Pulla<sup>a</sup>, Priyanka Suryadevara<sup>a</sup>, Keerthana Sharma Chennubhotla<sup>b</sup>, Pushkar Kulkarni<sup>b,c</sup>, Perumal Yogeewari<sup>a</sup>, Dharmarajan Sriram<sup>a,\*</sup>

<sup>a</sup> Department of Pharmacy, Birla Institute of Technology & Science-Pilani, Hyderabad Campus, Shameerpet, Jawahar Nagar, Ranga Reddy District, Hyderabad 500078, Andhra Pradesh, India

<sup>b</sup> Dr. Reddy's Institute of Life Sciences, University of Hyderabad Campus, Gachibowli, Hyderabad 500046, India

<sup>c</sup> Zephase Therapeutics (An Incubated Company at the Dr. Reddy's Institute of Life Sciences), University of Hyderabad Campus, Gachibowli, Hyderabad 500046, India

## ARTICLE INFO

## Article history:

Received 7 July 2014

Revised 3 September 2014

Accepted 5 September 2014

Available online xxxxx

## Keywords:

DNA gyraseB

Antibacterial activity

hERG inhibition

Biofilm

Cytotoxicity

## ABSTRACT

The gyraseB subunit of *Staphylococcus aureus* DNA gyrase is a well-established and validated target though less explored for the development of novel antimicrobial agents. Starting from the available structural information in PDB (3TTZ), we identified a novel series of benzimidazole used as inhibitors of DNA gyraseB with low micromolar inhibitory activity by employing structure-based drug design strategy. Subsequently, this chemical class of DNA gyrase inhibitors was extensively investigated biologically through in vitro assays, biofilm inhibition assays, cytotoxicity, and in vivo studies. The binding affinity of the most potent inhibitor **10** was further ascertained biophysically through differential scanning fluorimetry. Further, the most potent analogues did not show any signs of cardiotoxicity in Zebra fish ether-a-go-go-related gene (zERG), a major breakthrough among the previously reported cardiotoxic gyraseB inhibitors.

© 2014 Elsevier Ltd. All rights reserved.

## 1. Introduction

The Gram-positive bacterium *Staphylococcus aureus* was a normal flora, inhabiting 30% of human population, had emerged to the status of causative agent of many infections globally and was found to be a major cause of morbidity and mortality in community-associated environments and hospital settings.<sup>1,2</sup> According to the statistics, a gradual evolution of methicillin resistant strain of *S. aureus* (MRSA) seem to be a global threat accounting for about 50% death worldwide.<sup>3</sup> The available therapies no longer found effective in treating the infections due to increased antibiotic resistance, while the other failure for developing therapeutics to treat this gram-positive bacterial infections is due to the formation of biofilm compounded by the existence of multiple biofilm mechanisms in *S. aureus* and high resistant MRSA.<sup>4,5</sup> By implementing certain unique strategies like identifying novel therapeutic agents, that can inhibit the known drug targets through a unique binding site and also by following different strategy in drug inhibition

mechanisms like broad spectra of efficacy, reduced toxicity and improved ADME properties, could help in evading the existing bacterial resistance without side effects.<sup>6,7</sup>

DNA gyrase could be one such attractive target which possess the above features and could aid in developing antibacterial agents against the infectious organism.<sup>8</sup> Gyrase belongs to type II topoisomerase class from the GHKL (gyrase, HSP 90, histidine kinase, MutL) enzyme family that plays an important role in maintaining the DNA topology.<sup>7</sup> The main role of the enzyme is to introduce negative supercoils through ATP hydrolysis in the process of replication, unlike other topoisomerases, makes it a unique target in drug discovery.<sup>9</sup> It is a heterodimeric enzyme with A2B2 complex, the A subunit aid in breakage and reunion of the double stranded DNA, while the B subunit act through ATPase function, providing sufficient amount of energy for the DNA supercoiling.<sup>10</sup> Not many drugs acting through DNA gyrase are reported till date except 6-fluoroquinolone chemical class of molecules. These are the only DNA gyrase inhibitors approved and available for clinical practice.<sup>7</sup> The strategy of inhibition by the quinolones involves binding to the ternary complex formed between the DNA molecule and the DNA gyraseA subunit, subsequently stabilizing the complex. As a whole

\* Corresponding author. Tel.: +91 40663030506; fax: +91 4066303998.

E-mail address: [dsriram@hyderabad.bits-pilani.ac.in](mailto:dsriram@hyderabad.bits-pilani.ac.in) (D. Sriram).

this ternary complex helps in preventing the reunion of both the DNA strands and ultimately stopping the bacterial replication cycle. Fluoroquinolones have significant utility in the treatment of respiratory and urinary infections; however, the occurrence of some serious side effects calls for novel research in this field.<sup>11</sup> The other drawback of this chemical class is, they are more potent against the gram-negative bacteria when compared with gram-positive ones due to the presence of another homologous target topoisomerase IV.<sup>12</sup> In order to overcome these hindrances, we took efforts to explore on a less targeted side of DNA gyrase. That is the DNA gyraseB which is an ATP binding subunit, clinically very important as it holds the catalytic domain unlike the gyraseA subunit.<sup>13</sup> There are several natural and synthetic classes designed to inhibit gyraseB and were evaluated biologically, but none have come up to the final stages of clinical trials; though novobiocin being the only one released into the market in 1960s, was later withdrawn due to its toxicity and permeability issues.<sup>14,15</sup> Other reported gyraseB inhibitors include coumarins,<sup>16</sup> cyclothialidines,<sup>17</sup> pyrazolthiazoles<sup>18</sup> and pyrrolamides<sup>6</sup> classes which were rather unsuccessful due to their permeability parameters and their in vivo antibacterial activity. In the present study, we attempted development of a novel class of *S. aureus* DNA gyraseB inhibitors employing energy-optimized structure based pharmacophore (e-pharmacophore) as a query in database searching. The identified hits were procured and subjected to in vitro activity analysis, of which the top active lead was considered for synthesizing its derivatives. The working outline from design phase to the in vivo activity has been depicted in Figure 1.

## 2. Results and discussion

### 2.1. Design and chemistry

Our effort to identify novel small molecule inhibitors that bind to the active site of *S. aureus* gyraseB ATPase domain started with e-pharmacophore approach, which combined both the aspects of structure-based and ligand-based techniques using the crystal structure of DNA gyraseB protein-ligand complex (PDB code: 3TTZ)<sup>19</sup> as template. The pharmacophore hypothesis was established by mapping the energetic terms from the extra precision Glide scoring function (Glide XP) onto the atom centres (Glide, version 5.7, Schrödinger, LLC, New York, NY, 81 2011).<sup>20,21</sup> The structural and energetic information between the protein and ligand were evaluated by using Phase module (Phase, v3.3, Schrödinger, LLC, New York, NY). A three-point e-pharmacophore model was generated with ATPase gyraseB domain. The pharmacophoric sites established included one donor (D), one acceptor (A) and one negative ionisable group (N), which was further utilised for virtual screening of commercial database (Asinex) containing five lakh molecules using the protocol as described in Section 4.1. Initially, the compounds were retrieved by the three-point e-pharmacophore filter using phase module and those with fit value above 2 were regarded as potential hits and were further subjected to high throughput virtual screening. The top compounds having a good fitness, docking pose with two or more hydrogen bonds, with a Glide score  $\geq 5.8$  kcal mol<sup>-1</sup> were subjected to another round of docking by Glide XP. The Glide XP module has been reported to

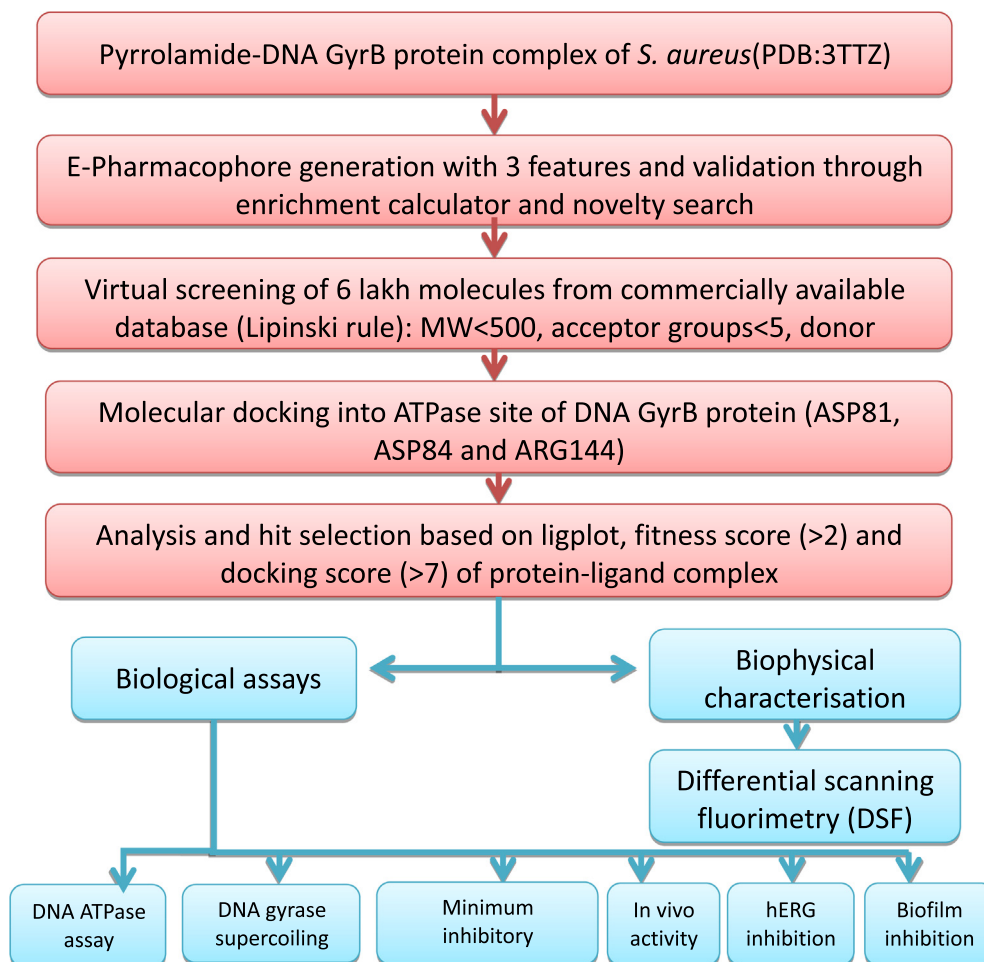


Figure 1. Outline of the computational and biological work presented in this study.

be a precise tool as it combines accurate, well defined physics-based scoring terms and thorough sampling of the terms. The final output file resulted in scores ranging from  $-11.81$  to  $-6.93$  kcal mol $^{-1}$ . The final shortlisting of the molecules was based on the protein ligand interaction in the active site cleft through hydrogen bonding with Asp81, Arg144 and via  $\pi$  stacking with-Arg84. GyraseB consisted of a hydrophobic pocket, surrounded by the amino acid residues like Ser55, Thr173, Val79, Gly85, Pro87, Glu58, Asn54, and Ile86 in the vicinity. Finally, top twelve hits were selected from the Asinex database and were evaluated biologically. Among the twelve hits shown in Figure 2 four compounds (BAS01340688, BAS01355130, BAS04380545, and BAS3776474) showed IC<sub>50</sub> of less than 20  $\mu$ M against gyraseB and others except one (BAS01340688) showed an IC<sub>50</sub> less than 100  $\mu$ M. All these compounds were also tested for the DNA supercoiling assay and only six compounds showed bioactivity

with IC<sub>50</sub> less than 50  $\mu$ M and the compounds BAS01340688, BAS01355130, BAS04380545 and BAS3776474 were found to be promising as revealed in the gyraseB inhibition assay. Among the active compounds, the hits BAS01340688 and BAS01355130 belong to benzimidazole nucleus and the most active compound was found to be 4-[4-(1*H*-benzimidazol-2-yl)-phenylcarbonyl] butanoic acid (BAS01355130), which showed significant activity in the gyraseB assay (IC<sub>50</sub> of  $12.6 \pm 0.32$   $\mu$ M) and supercoiling assay (IC<sub>50</sub> of 2.9  $\mu$ M). The docking orientation of this compound BAS01355130 hereafter represented as lead 1, when compared with the crystal ligand, revealed important polar contacts with Asp81, Arg84 and Arg144 similar to that of the crystal ligand of *S. aureus* gyraseB. The docking score of lead 1 was found to be  $-6.58$  and a strong non-polar interaction by the benzimidazole moiety at the adenine binding position of ATP with Ile51, Ile102 and Ile175 was observed as shown in Figure 3.

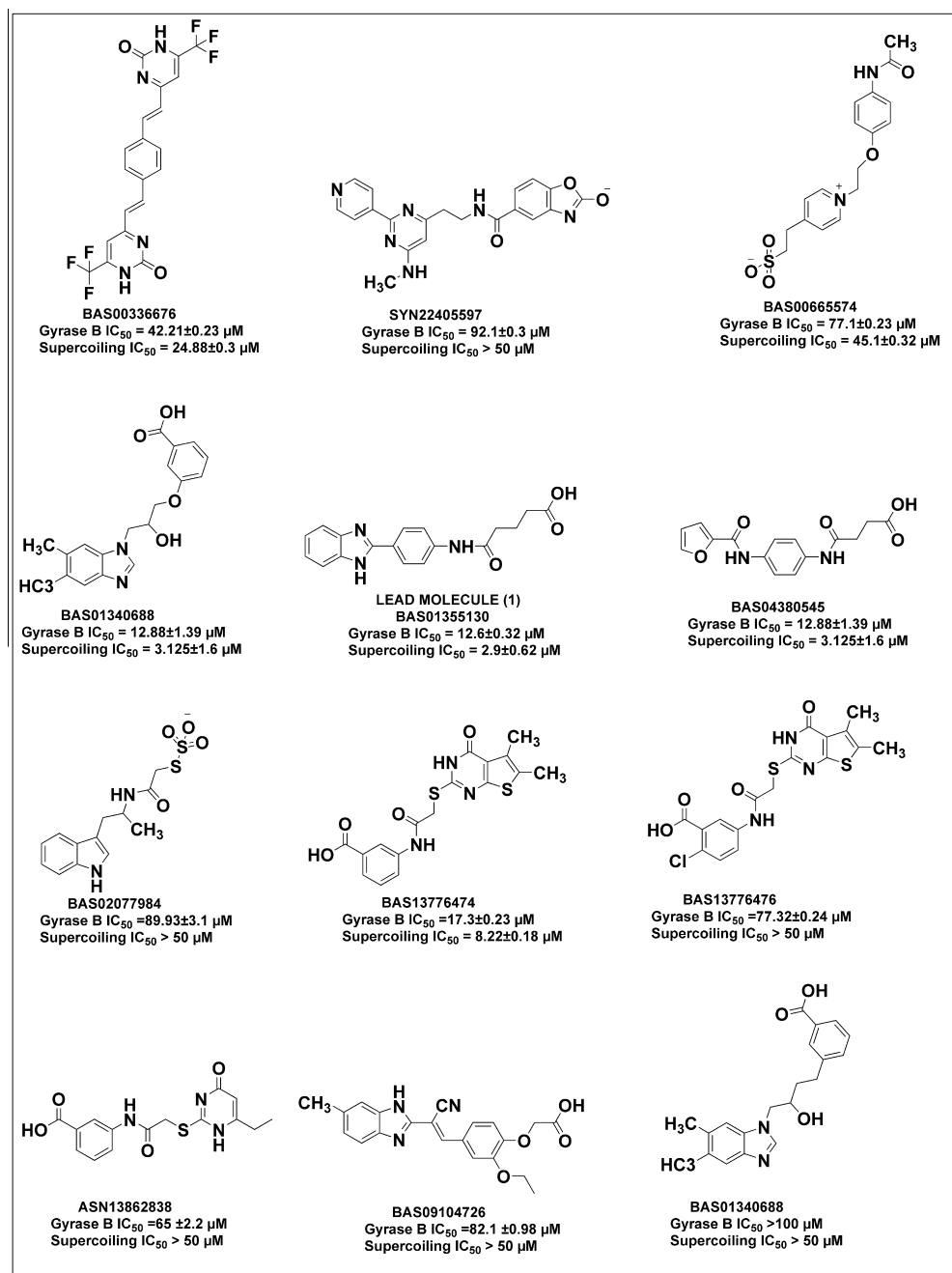


Figure 2. Top twelve hit molecules retrieved from Asinex database after virtual screening of 5 lakh molecules.

The lead molecule **1** (BAS01355130) has an benzimidazole nucleus on the left hand core that run through a 4-aminophenyl linker, to a right handed acyl side chain as per Figure 2. The promising results of the virtual screening hits encouraged us to design a library of benzimidazole scaffold with a goal of obtaining a series of analogues with tractable SAR and potencies better than the identified virtual screening lead. Considering the input from protein–ligand interactions observed with the crystal structure of gyraseB and the lead molecule **1**, the following modifications (and combinations thereof) were attempted as a first ligand expansion step which included (i) exploring the effect of various substituent's on benzimidazole nucleus (ii) extending the length of acyl side chain and converting the carboxylic acid group into their corresponding ester as shown in Table 1, to identify the ideal sites for introducing chemical diversity and to have a clearer understanding of the role of these substituent as determinants of inhibitory potency. The synthetic pathway used to achieve lead modifications is delineated in Scheme 1. The synthesis of target molecules began with the condensation of commercially available substituted 1,2 phenylenediamine (compounds **2a–e**) with 4-aminobenzoic acid in the presence of Eaton's reagent to yield the corresponding 4-(sub:-1*H*-benzo[d]imidazol-2-yl) aniline (compounds **3a–e**) in good yields. This method utilizing Eaton's reagent was highly beneficial in improving the yields of the so obtained 1*H*-benzo[d]imidazol-2-yl) aniline analogues, when compared to other reagents/protocols available in literatures. A similar strategy was adopted to develop 4-(3*H*-imidazo [4,5-*b*]pyridin-2-yl)aniline nucleus (**3f**) as well, starting from 1,2-diaminopyridine (**2f**). Functionalization of 4-aminophenyl linker was then brought about by treatment with various acid anhydrides to yield compounds **4–32**. Further the carboxylic acid side chains of few selected analogues (**5**, **10**, **15**, **20**, **25** and **30**) were converted into their corresponding esters (**6**, **11**, **16**, **21**, **26** and **31**) as an effort to improve the bacterial cell wall permeability of these compounds. The oxygen and thio-substituted acyl derivatives (**33–44**) were prepared by coupling 4-(sub:-1*H*-benzo[d]imidazol-2-yl)aniline/4-(3*H*-imidazo[4,5-*b*]pyridin-2-yl)aniline nucleus (**3a–f**) with diglycolic acid and 2,2'-thiodiacetic acid respectively. A library of forty one derivatives were synthesized (**4–44**, as shown in Table 1), characterized and evaluated for their ability to inhibit the gyraseB activity as an effort towards the derivatization of structure–activity relationships and lead optimization.

## 2.2. DNA gyraseB enzyme inhibition of synthesized compounds

As reported earlier, the purified *S. aureus* gyraseB do not have a highly active ATPase activity like *Escherichia coli* gyraseB.<sup>22</sup> As a

result, gyraseB assay was performed with recombinant proteins of *E. coli* gyraseA and *S. aureus* gyraseB.<sup>19,23</sup> A library of forty one compounds synthesized, were screened for the gyraseB activity, throughout the assay novobiocin was set as standard positive control with an IC<sub>50</sub> of 15 nM.<sup>9</sup> Among the forty one compounds tested, thirty two compounds showed a good inhibitory potency profile of >80% at 50 μM and 20 μM concentrations. Subsequently, these thirty two compounds were rescreened at lower concentrations of 10 μM and 5 μM, in which four compounds showing >65% inhibition. A final compound concentration of 1 μM for the four potent compounds was performed and IC<sub>50</sub> was calculated by GraphPad Prism software, evaluating the compounds in the above five concentrations for the final time in duplicates. The assay was performed in the presence of detergent to rule out the artifacts like auto absorbance and aggregation of molecules. The IC<sub>50</sub> are shown in Table 1.

In order to evaluate the binding profile and interaction pattern of the designed library of molecules, in silico molecular docking studies were carried out with the crystal structure of *S. aureus* gyraseB. With respect to the structure–activity relationship study; out of the various substitutions attempted on the benzimidazole nucleus, the 5-fluoro substituted analogues turned out to be more promising leads with compound **10** emerging as the most potent analogue with an IC<sub>50</sub> of 1.32 ± 0.17 μM as shown in Figure 4, which showed a 10 fold increment in activity when compared to the lead compound **1** (BAS01355130). The corresponding docking score of compound **10** was –7.06, better than that of lead compound **1** which showed –6.58; revealing a good binding affinity against the protein. Compound **10** was found to retain all the crucial polar contacts as that of crystal ligand (Asp81, Arg84 and Arg144) as illustrated in Figure 5. The remarkable potency of the compound **10** may be attributed to the presence of highly lipophilic fluorine attached to the benzimidazole group which was involved in strong in nonpolar interactions with residues Ile51, Ile102, Leu103 and Ile175 as conferred from docking study. The terminal carboxylic acid side chain as well as the chain length was detrimental to bioactivity as these modifications of the terminal carboxyl group into the corresponding methyl ester and alteration in linker chain length resulted in decreased activity as found in case of compounds **8**, **9**, **11** and **12**. Replacement of fluoro group in 5th position of the benzimidazole nucleus with chlorine atom resulted in compounds with reduced activity having an IC<sub>50</sub> in the range of 11.23 to 35.63 μM and docking score of –6.43 to –4.89. This reduced activity range can be attributed to the high electron affinity nature of chlorine. Though these compounds were found to possess polar contacts with Arg144, the presence of chlorine containing lone pair of electrons was believed to perturb

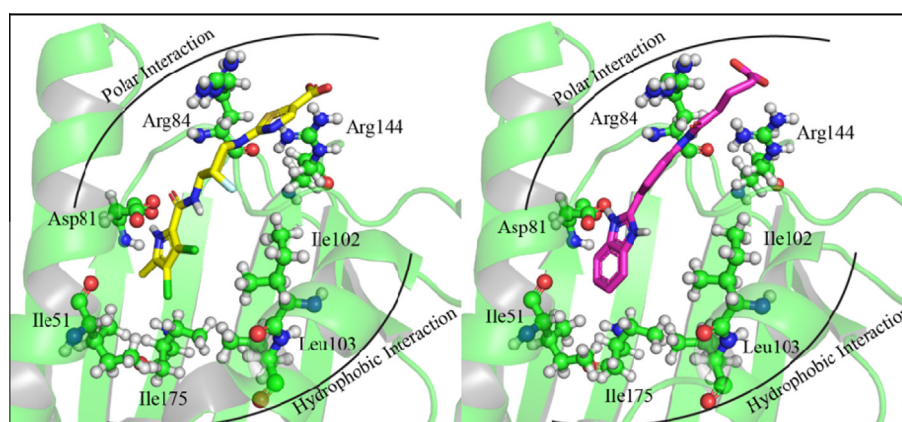
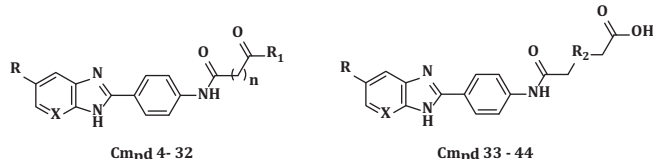


Figure 3. Interaction pattern of crystal ligand and lead molecule **1** (BAS01355130).

**Table 1**  
Biological evaluation of the synthesized compounds



Compd	R	n	X	R <sub>1</sub>	R <sub>2</sub>	GyraseB assay (IC <sub>50</sub> ) <sup>a</sup>	Supercoiling assay (IC <sub>50</sub> ) <sup>b</sup>	MIC (μM) <sup>c</sup>	MRSA MIC (μM) <sup>d</sup>	Biofilm Inhibi. (IC <sub>50</sub> ) <sup>e</sup>	Cytotoxicity (% inhibi.) <sup>f</sup>
4	H	1	H	OH	—	6.91 ± 0.43	6.125 ± 0.21	42.33	21.16	47.8	7.2
5	H	2	H	OH	—	7.32 ± 0.83	6.125 ± 0.32	20.205	40.41	88.31	2.9
6	H	3	H	OCH <sub>3</sub>	—	36.31 ± 0.48	25 ± 0.37	148.2	148.2	>100	9.7
7	H	4	H	OH	—	5.7 ± 0.16	6.125 ± 0.44	37.05	37.05	81.5	32.06
8	F	1	H	OH	—	13.43 ± 1.12	16.31 ± 0.21	79.8	79.8	>100	18.06
9	F	2	H	OH	—	17.6 ± 0.87	12.0 ± 0.26	38.19	38.19	82.7	28.72
10	F	3	H	OH	—	1.32 ± 0.17	1.13 ± 0.34	4.57	9.15	9.63	7.59
11	F	3	H	OCH <sub>3</sub>	—	18.6 ± 0.56	10.7 ± 0.11	70.35	32.175	59.33	33.81
12	F	4	H	OH	—	15.34 ± 0.32	7.1 ± 0.11	35.17	59.3	>100	29.04
13	Cl	1	H	OH	—	26.35 ± 0.23	18.21 ± 0.71	75.8	75.8	>100	25.62
14	Cl	2	H	OH	—	11.23 ± 0.85	9.8 ± 0.34	36.36	36.36	53.2	31.66
15	Cl	3	H	OH	—	9.85 ± 0.31	9.13 ± 0.11	34.9	69.8	>100	45.52
16	Cl	3	H	OCH <sub>3</sub>	—	35.63 ± 0.76	22.19 ± 1.56	67.23	134.47	>100	27.93
17	Cl	4	H	OH	—	13.06 ± 1.73	8.91 ± 0.35	33.61	33.61	39.2	39.67
18	NO <sub>2</sub>	1	H	OH	—	4.932 ± 0.34	2.23 ± 0.51	9.18	18.33	18.35	26.91
19	NO <sub>2</sub>	2	H	OH	—	17.53 ± 1.41	8.32 ± 0.77	16.96	16.96	27.92	24.57
20	NO <sub>2</sub>	3	H	OH	—	6.832 ± 0.49	6.12 ± 0.18	33.9	44.12	62.31	27.23
21	NO <sub>2</sub>	3	H	OCH <sub>3</sub>	—	9.83 ± 1.1	5.3 ± 0.25	32.69	32.69	59.31	35.89
22	NO <sub>2</sub>	4	H	OH	—	9.823 ± 0.61	6.09 ± 0.42	32.6	44.2	52.2	31.74
23	OCH <sub>3</sub>	1	H	OH	—	11.06 ± 0.23	18.36 ± 0.33	38.42	76.84	>100	27.35
24	OCH <sub>3</sub>	2	H	OH	—	13.43 ± 0.85	11.3 ± 0.48	73.67	73.67	>100	26.74
25	OCH <sub>3</sub>	3	H	OH	—	8.93 ± 0.44	5.32 ± 0.17	35.37	35.37	52.2	22.37
26	OCH <sub>3</sub>	3	H	OCH <sub>3</sub>	—	21.34 ± 0.34	12.5 ± 0.67	68.04	34.02	63.9	50.48
27	OCH <sub>3</sub>	4	H	OH	—	22.93 ± 1.33	12.5 ± 0.71	68.04	34.08	71.1	29.36
28	H	1	N	OH	—	21.8 ± 0.94	8.9 ± 0.38	42.18	42.18	71.9	27.24
29	H	2	N	OH	—	9.23 ± 0.88	3.125 ± 0.61	20.14	10.07	29.43	31.14
30	H	3	N	OH	—	18.53 ± 1.44	6.98 ± 0.67	38.54	38.54	88.09	33.81
31	H	3	N	OCH <sub>3</sub>	—	5.23 ± 0.81	6.8 ± 0.1	36.94	36.94	79.32	57.54
32	H	4	N	OH	—	2.9 ± 0.4	2.1 ± 0.23	4.61	9.23	15.73	22.72
33	H	—	H	—	O	6.01 ± 0.41	4.81 ± 0.41	38.42	46.88	68.8	40.02
34	H	—	H	—	S	22.8 ± 0.14	12.5 ± 0.82	73.3	37.6	82.1	13.07
35	F	—	H	—	O	6.125 ± 0.23	2.9 ± 0.31	9.102	9.102	19.64	14.47
36	F	—	H	—	S	6.93 ± 0.83	4.8 ± 0.54	34.78	17.32	59.12	20.63
37	Cl	—	H	—	O	15.34 ± 0.88	12.5 ± 0.92	34.74	69.49	71.23	29.67
38	Cl	—	H	—	S	13.83 ± 0.62	12.1 ± 0.95	4.15	4.15	9.72	23.04
39	NO <sub>2</sub>	—	H	—	O	8.51 ± 0.54	5.8 ± 0.31	33.75	46.98	83.22	31.29
40	NO <sub>2</sub>	—	H	—	S	3.132 ± 0.24	2.1 ± 0.31	8.087	16.98	10.32	25.21
41	OCH <sub>3</sub>	—	H	—	O	4.34 ± 0.77	3.062 ± 1.53	17.58	17.58	31.72	23.26
42	OCH <sub>3</sub>	—	H	—	S	9.31 ± 0.63	15.98 ± 0.28	67.31	67.31	>100	22.63
43	H	—	N	—	O	6.935 ± 0.25	4.7 ± 0.52	19.15	38.3	82.45	38.71
44	H	—	N	—	S	2.31 ± 0.48	1.7 ± 0.3	4.55	9.12	11.31	31.86
	Novobiocin					0.125 ± 0.24	0.030 ± 0.015	0.25	ND	ND	ND

ND, indicates not determined.

<sup>a</sup> *S. aureus* gyraseB ATPase activity.

<sup>b</sup> *S. aureus* DNA gyrase supercoiling activity.

<sup>c</sup> In vitro (MTCC 3160) activity.

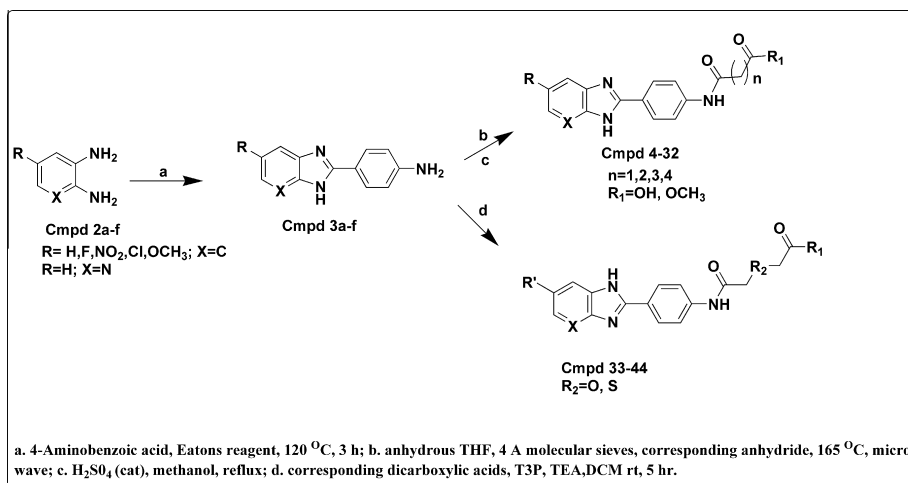
<sup>d</sup> In vitro (MTCC 96) MRSA MIC activity.

<sup>e</sup> Biofilm inhibition of MTCC 96.

<sup>f</sup> At 100 μM against RAW 264.7 cells.

the electron cloud spanning over the aromatic ring, thereof resulting in the loss of key non-polar interactions in the binding pocket. Another important factor playing a key role in the reduced activity profile of these compounds can be the steric hindrance imparted by chlorine. The bigger size of chlorine in comparison to fluorine can be attributed for the decreased activity of the compounds as chlorine blocks the efficient binding of compounds at the active site. However nitro substitution at 5th position of benzimidazole nucleus (**18–22**, **39**, **40**) resulted in compounds showing good activity profile with IC<sub>50</sub> in the range of 3.13–17.53 μM. Docking studies in this case conferred that the presence of nitro group on benzimidazole increased the non-polar interactions at the

hydrophobic pocket and an additional polar contact with Asn54 which explains their activity. Introduction of sulfur in the linker chain (**40**) made the compound more active probably due to an extra polar contact that it maintained with Arg144. Decrease in the linker length to one carbon chain as in compound **18** (docking score of –6.2) oriented the molecule in the vicinity of Arg144 allowing the two carbonyl oxygen to healthier interactions. Substitution of methoxy group at 5th position of benzimidazole nucleus (**23–27**, **41** and **42**) was found to reduce the activity profile against GyrB with IC<sub>50</sub> in the range of 4.34–22.93 μM. Presence of methoxy group resulted in less active compounds owing to its nature of stearic bulkiness, and was not involved in any non-polar



**Scheme 1.** Synthetic protocol adopted for the lead derivatization.

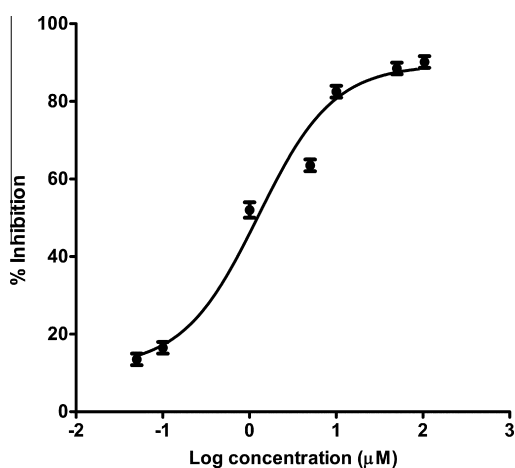


**Figure 4.** Hill slope of compound **10** with different log concentration of the inhibitor on X-axis against percentage inhibition on Y-axis.

interactions. However, compound **41** was found to be active with IC<sub>50</sub> of 4.34 µM and docking score of  $-7.09$ , probably due to the introduction of oxygen in linker which made the compound to orient in such a way that the two carbonyl oxygen made polar contact with Arg144. Also methoxy group was found to be involved in polar contact with Ser129 attributing to its better activity profile. Compounds **25** and **42** were found to retain the polar contacts with Asp81 and Arg144 with scores of  $-7.1$  and  $-6.72$ , respectively. From the combined inference from assays and docking studies, it implied that as observed in earlier cases, the linker length played an important role in the methoxy substituted series as well as a decrease in linker length also was detrimental to activity. Replacement of benzimidazole nucleus with imidazopyridine (**28–32**, **43** and **44**) was found to be beneficial resulting in compounds with marked activity in the range of 2.9–21.8 µM. Further, introduction of sulfur in the side chain linker (as modifications over compound **44**), resulted in compounds with encouraging potency which was confirmed by docking where the compound orientated (thio substituted linker) into the hydrophobic pocket and imidazopyridine was towards the solvent exposure area. This

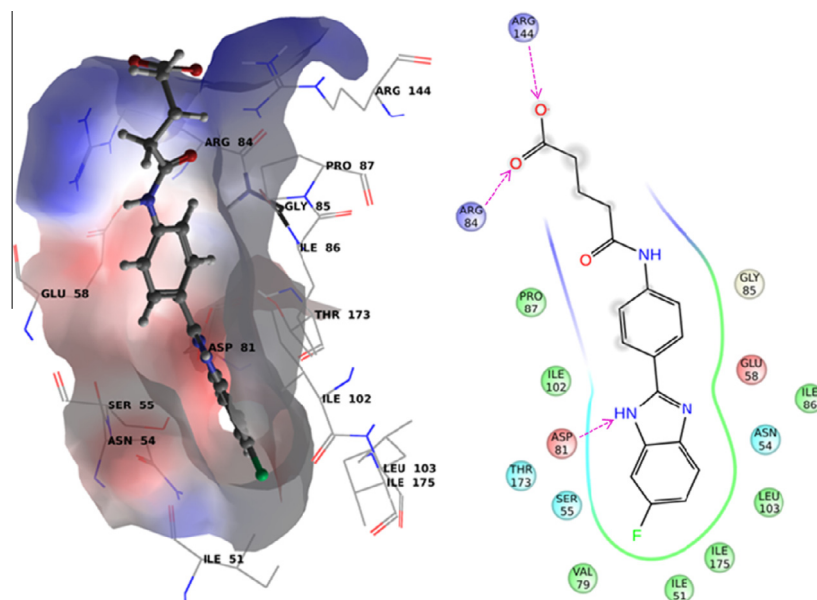


**Figure 5.** Surface interaction picture of Compound **10** with conserved amino acids accordance with ligand interaction diagram.

reorientation was acquired with an extra polar contact with Gly85 along with Asp81 and Arg144. Compound **32** (docking score of  $-6.89$ ), the only potent compound with increased linker length (four carbon chain) was found with its imidazopyridine in the hydrophobic pocket and the terminal carboxyl group interacting with Arg84 and Arg144. Presence of terminal methyl-ester moiety as in compound **31** (docking score of  $-6.72$ ) was also found to have a similar interaction profile.

In a nutshell, it can be concluded that substitutions like fluoro and nitro groups on benzimidazole were favorable in terms of activity against *S. aureus* gyraseB. The linker length played an important role in the activity as it was found to be involved in the orientation of the terminal hydrophobic and hydrophilic moieties in the active site. Linker length of three carbon atoms was found to be favorable in many of the cases and four carbon chains was tolerated in few cases as illustrated above. Decrease in linker length was not recommended, as these compounds showed a marked reduction in activity. Presence of oxygen and sulfur were advantageous with few compounds as they were involved in the orientation of the compound at the active site for interactions.

### 2.3. DNA supercoiling assay

Supercoiling of the DNA occurs in the presence of gyraseA and gyraseB subunits. Targeting either of the domains may result in loss of supercoiling activity. The DNA supercoiling assay was performed using a commercially available Inspiralis kit (Inspiralis Limited, Norwich, UK) with a positive control, moxifloxacin having an  $IC_{50}$  of  $11.2 \pm 1.8 \mu\text{M}$ .<sup>24</sup> The kit included the assay buffer, relaxed pBR 322 DNA as substrate, *S. aureus* DNA with A2B2 subunits. A library of the above forty one synthesized compounds when screened initially at  $50 \mu\text{M}$  and  $25 \mu\text{M}$  concentrations, we found thirty nine compounds with percentage inhibition  $>60\%$ . These compounds were repeated at lower concentrations of  $12.5 \mu\text{M}$  and  $6.25 \mu\text{M}$  subsequently, resulting in eleven compounds that exhibited  $>50\%$  relative inhibition profile. These potent inhibitory compounds were finally screened at  $1.56 \mu\text{M}$  and  $0.75 \mu\text{M}$  and  $IC_{50}$  values are reported in Table 1. As observed in the gyraseB assay results, compound **10** was found to be the most potent exhibiting an  $IC_{50}$  value of  $1.13 \pm 0.34 \mu\text{M}$  as depicted in Figure 6. Thus the gyraseB assay results well correlated with the supercoiling activity profile.

### 2.4. In vitro MIC evaluation

All the synthesized compounds (**4–44**) were further tested for their in vitro antibacterial activity against two bacterial strains, *S. aureus* MTCC 3160 and MRSA 96 using the protocol as described in Section 4.3.4. Ofloxacin and ciprofloxacin were included as reference compounds. The results of the antibacterial screening are presented in Table 1. Compound **10** which displayed a very good

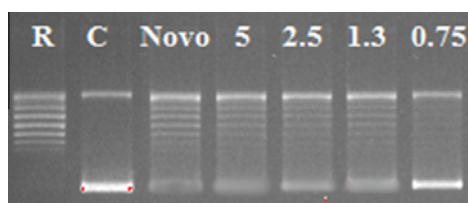


**Figure 6.** Inhibitory profile of *S. aureus* DNA gyrase supercoiling activity by compound **10**. A representative gel obtained from the analysis of the inhibition of DNA gyrase supercoiling activity is shown above. (R) represents relaxed closed circular DNA; (C) represents the supercoiled relaxed DNA in the presence of gyrase enzyme. Gel data for assays with compound **10** in different concentrations with novobiocin as positive standard are shown (in  $\mu\text{M}$ ).

enzyme inhibition also displayed significant in vitro antibacterial activity against both the MTCC and MRSA strains indicating its potential as bactericidal in vitro, whose MICs were  $4.57 \mu\text{M}$  and  $9.15 \mu\text{M}$  comparable to the reference compound ofloxacin which showed  $4.15 \mu\text{M}$  and  $17.29 \mu\text{M}$  in MTCC 3160 strain and MRSA 96 strain respectively. Ciprofloxacin displayed an MIC of  $9.431 \mu\text{M}$  against MTCC 3160 and  $18.8 \mu\text{M}$  against MRSA strain. This confirmed the activity profile of the compound **10** with respect to the reference standards ofloxacin and ciprofloxacin as bactericidal. Compounds **38** and **44** also exhibited good antimicrobial properties in both the strains highlighting the efficacy of this chemical class of molecules in inhibiting the microbes. In contrast, few compounds **5–9**, **13–17**, **25–28** and **43** displayed a weak antibacterial activity against the above bacterial strains, which could be attributed to the permeability issue or efflux pump transportation.

### 2.5. Inhibition of biofilm formation by *S. aureus*

Biofilm is an extracellular polysaccharide, produced by staphylococcal species that facilitate attachment and matrix formation that results in alteration in the phenotype of the organism, with respect to gene transcription and growth rate.<sup>25</sup> It was estimated that 65% of all the human bacterial infections were due to biofilm formation which may result in prolonged and chronic infections leading to death.<sup>25,26</sup> While recalcitrance of these biofilm-mediated infections has been associated with adverse effect on patient health, the increase in the resistance of *S. aureus* to methicillin resulted in more hysterical condition.<sup>27</sup> The extensive resistance of *S. aureus* biofilms against the antibacterials can be attributed to failure of antibiotics to penetrate the biofilm, the different metabolic states of the cells in the biofilm aggregates, and the differential expression of genes by the bacteria concerned in the same biofilm aggregates.<sup>28</sup> One of the novel approach of inhibiting pathogen virulence could be by inhibiting the biofilm formation thus minimizing the selection pressure for resistance as it hold a great promise as an alternative to traditional antibiotic treatment.<sup>29</sup> We focused our study on inhibition of *S. aureus* biofilm formation by the forty one synthesised small molecule inhibitors. The estimation of inhibition of biofilm formation was monitored quantitatively and qualitatively. Initially, Congo red method was adopted to know the strain's efficiency in biofilm formation.<sup>27</sup> The MRSA 96 was a strong biofilm producer with  $>2$  OD at 570 nm wavelength. Assays were performed in a 96-well microtiter plate,

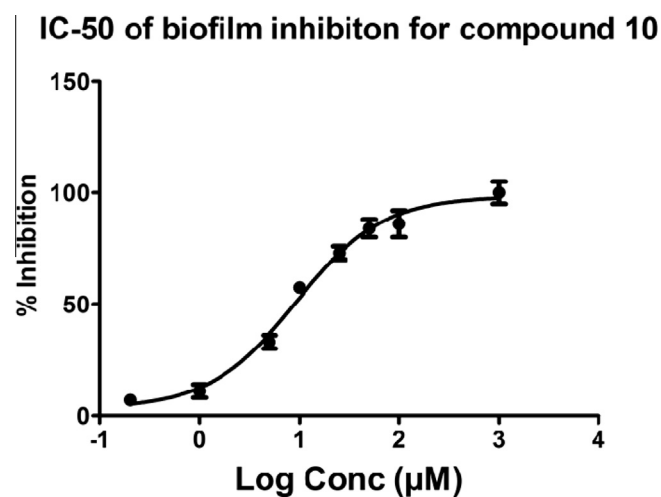


**Figure 7.** Dose–response curve of compound **10** inhibition on *S. aureus* MRSA 96 biofilm formation. The data is presented as% inhibition mean  $\pm$  standard error of means for 6 samples. Percent inhibition is relative to DMSO control.

with different concentrations of the compounds on biofilm producing clinical MRSA strain 96. The procedure followed was as illustrated in Section 4.3.5.1. All the forty one compounds were subjected for biofilm assay and it was gratifying to observe that the most potent compound **10** had good biofilm formation inhibitory profile with an  $IC_{50}$  of 9.63  $\mu$ M as shown in Figure 7. Ciprofloxacin was used as the standard reference possessing an  $IC_{50}$  of 16.89  $\mu$ M. In comparison with ciprofloxacin, compound **10** showed two-fold increased efficacy in inhibiting the biofilm formation. Compounds **39**, **19**, **33**, **36**, **41** and **45** also displayed appreciable  $IC_{50}$ 's below 20  $\mu$ M as depicted in Table 1, giving enough proof that this class of compounds possess dual effect, as DNA gyrase inhibitors with effective inhibition of biofilm formation too.

## 2.6. Cytotoxicity screening

Further to know the safety profile of this chemical class, forty one compounds were evaluated by testing for their in vitro cytotoxicity against mammalian HEK-293 cell line at 100  $\mu$ M concentration in triplicates by utilizing (4,5-dimethylthiazol-2-yl)-2,5-diphenyltetrazolium bromide (MTT) assay.<sup>30</sup> The entire series of compounds tested demonstrated a good safety profile range with very low inhibitory potential. These results were gratifying for us as the most potent compound **10** showed only 7% cytotoxicity at the highest concentration tested on par with ciprofloxacin drug which was considered as control and thus these results confirmed the safety profile of compounds. Percentage inhibition of HEK cells by all the forty one compounds is reported in Table 1.

## 2.7. In vivo evaluation in mouse septicaemia model

Based on the promising profile of compound **10**, in vivo efficacy was carried out in mouse septicaemia model. Briefly CD-1 female mice (10 per group) were administered *S. aureus* inoculum of  $3 \times 10^7$  cfu/mouse via intraperitoneal route. Mice were then treated with compound **10** in varying doses of 5, 10, and 25 mg/kg (iv) at time of and 4 h of post infection. Vancomycin was used as a control and dosed at 5 mg/kg. Survival was assessed 24 h post infection. Compound **10** was found to protect 60% of animals at 5 mg/kg, 80% and 100% protection at 10 and 25 mg/kg respectively as illustrated in Figure 8.

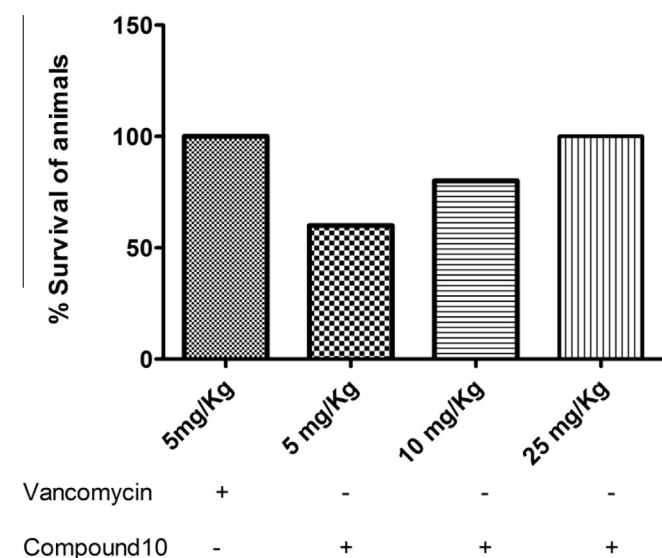


Figure 8. Number of survivals of mice, 24 h post infections with *S. aureus* treated with varying doses of compound **10**; standard drug was vancomycin.

## 2.8. hERG channel inhibition studies

Till date the only drugs clinically approved for DNA gyrase inhibition were fluoroquinolones, among which the potent one being moxifloxacin, that suffer from hERG toxicity.<sup>31,32</sup> Also the previously reported antibacterial C- and N-linked aminopiperidine DNA gyrase inhibitors suffered from serious hERG toxicity, we felt it was very important to ensure that the newly designed molecules did not suffer from such drawbacks. Compound **10** was subjected for hERG channel inhibition studies by assessing the arrhythmogenic potential on zebra fish ether-a-go-go-related gene (zERG) which was orthologous to the human ether-a-go-go-related gene (hERG), due to their homology. This method of study, possessed significant advantage over the current conventional animal models which include ethical issues, low compound requirement, manually less tedious and low cost. Presently, zebrafish (*Danio rerio*) has become an emerging model to study the pro-arrhythmic potential of candidate drugs.<sup>33</sup> Furthermore, Milan et al.<sup>34</sup> and Mittelstadt et al.<sup>35</sup> had reported that bradycardia and atrio-ventricular dissociation in zebrafish larvae can be used as a surrogate marker for hERG channel inhibition thereby affecting the rapid component of the repolarizing potassium current and inducing arrhythmia. In our study, compound **10** was subjected to hERG channel inhibition in concentrations ranging from 1  $\mu$ M to 30  $\mu$ M with 0.1% DMSO as vehicle, the heart rate variations and AV ratio were analysed by using a protocol described in more detail in Section 4.3.8. Compound **10** was found to be safe when compared to the positive control (20  $\mu$ M terfenadine), by not showing any significant cardiotoxicity until 30  $\mu$ M concentration. There was no significant change in the heart rate or AV ratio, in comparison to control group making them relatively safe, a significant breakthrough when compared to otherwise cardiotoxic terfenadine and amiodarone as illustrated in Figure 9a and b.

## 2.9. QikProp results

Further, to analyse various pharmacokinetic properties of these forty one compounds QikProp 3.5 module of Schrodinger software was utilized. A preliminary examination of the ADMET results showed that all the desired hits obey Lipinski's rule of five showing their drug-like nature. Compounds with favourable activity against *S. aureus* DNA gyraseB (**10**, **44**, **41** and **32**) showed parameters

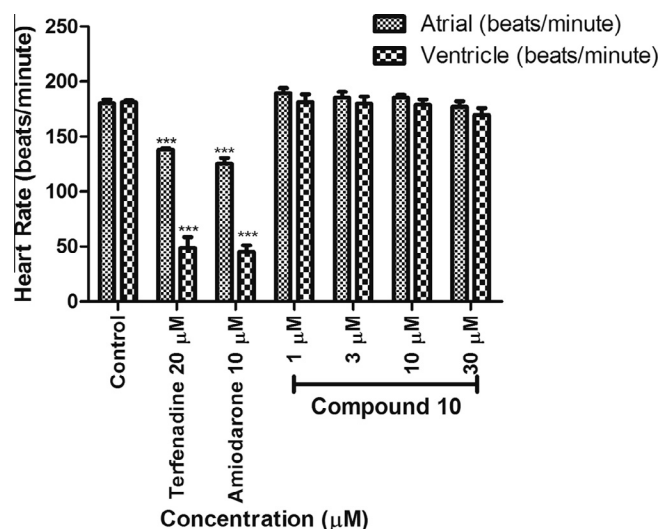
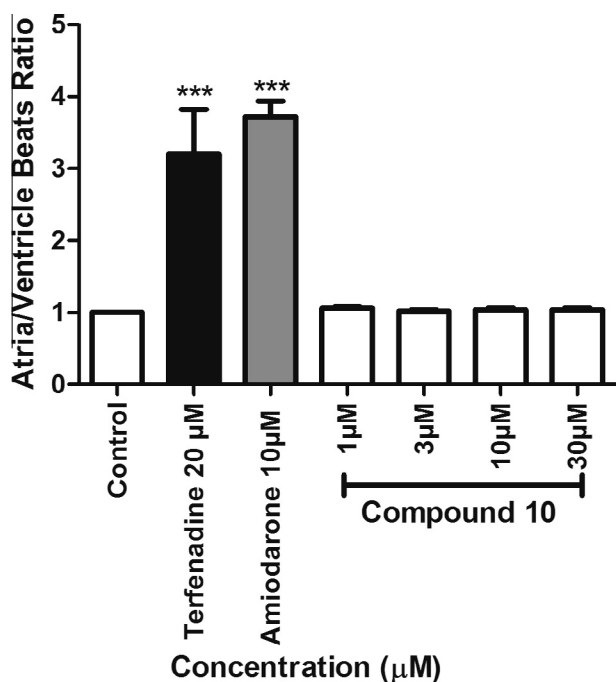


Figure 9a. Mean ( $\pm$ SEM) of the heart rates of atria and ventricles of Compound-**10**. (\* $p$  < 0.05, \*\* $p$  < 0.01 and \*\*\* $p$  < 0.001). Statistical significance was analyzed comparing control group versus treated groups.



**Figure 9b.** Mean ( $\pm$ SEM) score of atrio ventricular ratio. (\* $p$  < 0.05, \*\* $p$  < 0.01 and \*\*\* $p$  < 0.001). Statistical significance was analyzed comparing control group versus all groups.

within desirable range as shown in the [Supplementary information Table 1](#). Interestingly the inactive compound **6** showed poor range values for QPPCaco and QPPMDCK properties. As these two properties were important pharmacokinetic determining parameters for absorption and distribution fate of any drug-like compound. Additionally, percentage human oral absorption range was upto the mark for all active compounds considered, whereas compound **6** values were unacceptable for oral absorption. Thus according to the ADMET analysis, we can conclude that all the active compounds showed characteristics of a promising drug candidature which can be worked for rational drug design against *S. aureus* DNA gyraseB enzyme from pharmaceutical point of view.

## 2.10. Biophysical characterization

The active compounds from this series of chemical class of molecules were further investigated using a biophysical technique, differential scanning fluorimetry (DSF). The ability of the compounds to stabilize the catalytic domain of the gyrase protein was assessed utilizing the DSF technique by which the thermal stability of the catalytic domain of gyraseB native protein and of the protein bound with the ligand was measured.<sup>7,36</sup> Complexes with three different ligands **10**, **32** and **44** were heated stepwise from 25 °C to 95 °C in steps of 0.6 °C in the presence of a fluorescent dye, whose fluorescence increased as it interacted with hydrophobic residues of the gyraseB protein. As the protein was denatured, the amino acid residues became exposed to the dye.<sup>9</sup> A right side positive shift of  $T_m$  in comparison to native protein meant higher stabilization of the protein–ligand complexes, which was a consequence of the inhibitor binding.<sup>36</sup> In our study, compound **10** showed significant positive shift confirming the stability of the protein–ligand complex, as it was already reported in literature that the carboxylic group at *para* position played an important role in the complex stabilization by interacting with amino acid residues like Arg144, Arg84 as shown in our in silico model. In addition, the hydrophobic pocket formed around the lipophilic group by Ile102, Ile86, Leu103, Gly85, Ile102, Thr173, Ile175, Ile51 and Pro87 also contributed to the stabilization of this complex. Among the three tested compounds, best improvement in the protein–inhibitor complex stability, as indicated by the positive shift was observed in the case of compound **10** with the  $T_m$  shift of 3.2 °C, followed by compound **32** and **44**. These results were in accordance with the most potent DNA gyraseB inhibition by compound **10**, with an  $IC_{50}$  of  $1.32 \pm 0.17 \mu\text{M}$ . [Figure 10](#) depicts the curves obtained in the DSF experiment for the native gyraseB protein (red) and protein–compound **10** complex (blue).

## 3. Conclusion

Efforts since 1950s to discover a drug against DNA gyraseB enzyme have not been fruitful as there is no single drug approved clinically till date.<sup>7</sup> So in an effort to discover lead molecules against this enzyme, we generated a structure-based e-pharmacophore model to identify structurally diverse, small molecule

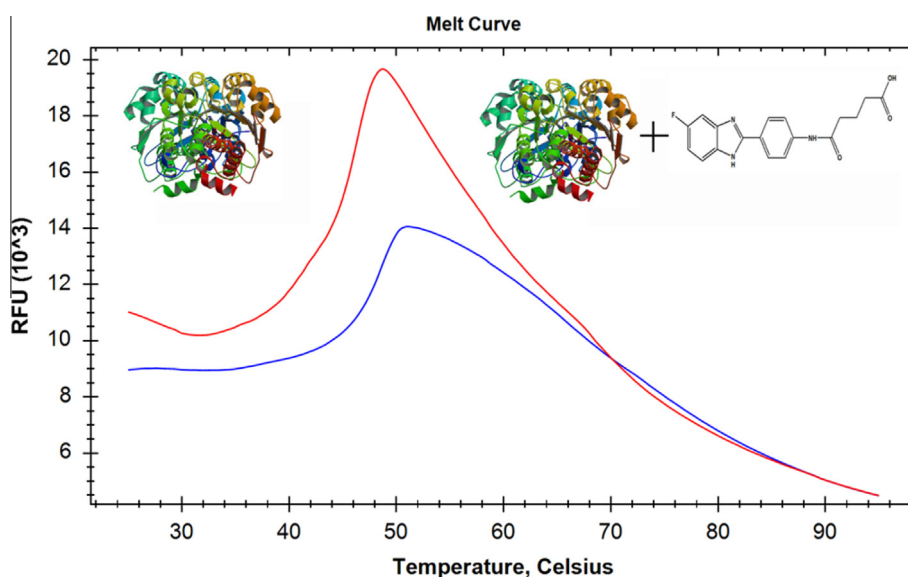


**Figure 10.** DSF experiment for compound **10** showing an increase in thermal stability between the native G24 protein (blue) and DNA gyraseB protein–compound **10** complex (red).

inhibitors of *S. aureus* DNA gyraseB enzyme based on the crystal structure of the enzyme with a co-crystallized inhibitor. Subsequently, twelve active compounds of varied structural classes were identified. Out of which, three molecules had an in vitro gyraseB activity in 5  $\mu\text{M}$  range, and the best compound was selected as lead **1** for which further synthesis of a library of forty one molecules was carried out. All these compounds were subjected to DNA gyraseB assay, DNA supercoiling assay, further their binding mode was biophysically confirmed by differential scanning fluorimetry (DSF). It was gratifying to see the best inhibitory compound **10** in the in vitro assays also showed a greater positive shift in DSF, indicating the highest increase of thermal stability of the complex inhibitor-protein that matched the best in vitro antimicrobial activity against the MRSA strain as well. Furthermore, compound **10** showed better biofilm inhibition profile along with low cell cytotoxicity in mammalian HEK-293 cell line with zero hERG inhibition posing no cardiotoxicity at all and a very high in vivo efficacy in the mouse model too, thereby making this compound a potent molecule in this chemical class of DNA gyraseB inhibitors. Furthermore, this class of benzimidazole besets a collection of promising lead compounds for further optimization and development to yield best novel drugs aimed to combat ever-present and ever-increasing bacterial infections. Undoubtedly, this study provides the basis for further chemical optimization of these potent inhibitors against DNA gyraseB enzyme.

## 4. Experiments

### 4.1. Computer aided structure-based pharmacophore model generation and virtual screening procedure

The crystal structure of *S. aureus* had co-crystallised inhibitor–DNA gyraseB protein complex was retrieved from Protein Data Bank (PDB code: 3TTZ), the interactions of the protein ligand were examined using the Schrodinger software. The module PHASE 3.3 implemented in the Maestro 9.2 software package (Schrodinger, LLC) was used to derive the e-pharmacophore. Glide energy grids were generated for each of the prepared complexes of protein–ligand. The binding site was defined by a rectangular box of 20 Å surrounding the ligand in the X-ray structure while the others were kept at default setting. Ligands were refined using the 'Refine' option in Glide, and the Glide XP (extra precision) descriptor was chosen (Glide v5.7, Schrodinger, LLC, New York, NY). Default settings were used for the refinement and scoring of the protein–ligand complex. The final model generated for the first phase of high throughput virtual screening consisted of a hydrogen bond donor, a ring group and a negative ionisable group.

### 4.2. Chemistry

All commercially available chemicals and solvents were used without further purification. TLC experiments were performed on alumina-backed silica gel 40 F254 plates (Merck, Darmstadt, Germany). The homogeneity of the compounds was monitored by thin layer chromatography (TLC) on silica gel 40 F254 coated on aluminum plates, visualized by UV light and  $\text{KMnO}_4$  treatment. Flash chromatography was performed on a Biotage Isolera with pre-packaged disposable normal phase silica columns. All  $^1\text{H}$  and  $^{13}\text{C}$  NMR spectra were recorded on a Bruker AM-300 (300.12 MHz, 75.12 MHz) NMR spectrometer, Bruker BioSpin Corp, Germany. Chemical shifts are reported in ppm ( $\delta$ ) with reference to the internal standard TMS. The signals are designated as follows: s, singlet; d, doublet; dd, doublet of doublets; t, triplet; m, multiplet. Molecular weights of the synthesized compounds were checked by LCMS 6100B series Agilent Technology. Elemental analyses were carried

out on an automatic Flash EA 1112 Series, CHN Analyzer (Thermo). The purity of the final compounds was examined by HPLC (Shimadzu, Japan, (on Phenomenex C8 (150 \* 4.6 mm, 5  $\mu\text{m}$ , 100 Å) double end-capped RP-HPLC column)) and was greater than 95%.

#### 4.2.1. General procedure for the synthesis of 4-(sub-1H-Benzo[d]imidazol-2-yl)aniline (3a–e)/4-(3H-imidazo[4,5-b]pyridin-2-yl)aniline (3f). procedure A

Eaton's reagent (10 vol; wt/vol) was added drop wise to a well pulverised mixture of the corresponding 1,2-phenylenediamine (**2a–e**)/1,2-diaminopyridine (**2f**) (1 equiv) and 4-amino benzoic acid (1 equiv) at 0 °C. The reaction mixture was then heated at 130 °C for 5–6 h (monitored by TLC and LCMS for completion). The reaction mixture was cooled and neutralised with 10% sodium hydroxide solution to pH of 6–7, the precipitate formed was filtered and washed repeatedly with water and dried. The solid obtained was recrystallized from ethanol to afford the desired product in good yield as described below.

#### 4.2.2. General procedure for the synthesis of 4-(1H-benzo[d]imidazol-2-yl)aniline (3a)

The compound was prepared according to the general procedure A using 1,2-phenylenediamine **2a** (1 g, 9.25 mmol), 4-amino benzoic acid (1.27 g, 9.25 mmol) and eatons reagent (10 mL) to afford **3a** (1.42 g, 74% yield) as pale brown solid. Mp: 259–261 °C.  $^1\text{H}$  NMR (DMSO- $d_6$ ):  $\delta_{\text{H}}$  6.42 (s, 2H), 6.82–7.98 (m, 8H).  $^{13}\text{C}$  NMR (DMSO- $d_6$ ):  $\delta_{\text{C}}$  153.1, 145.4, 141.5, 128.7, 123.5, 116.7, 115.5. EI-MS  $m/z$ : 210.45 (M+H) $^+$ . Anal. Calcd for  $\text{C}_{13}\text{H}_{11}\text{N}_3$ : C, 74.62; H, 5.30; N, 20.08. Found: C, 74.64; H, 5.33; N, 20.12.

#### 4.2.3. General procedure for the synthesis of 4-(5-fluoro-1H-benzo[d]imidazol-2-yl)aniline (3b)

The compound was prepared according to the general procedure A using 4-fluoro-1,2-phenylenediamine **2b** (1 g, 7.93 mmol), 4-amino benzoic acid (1.09 g, 7.93 mmol) and eatons reagent (10 mL) to afford **3b** (1.02 g, 56% yield) as brown solid. Mp: 242–244 °C.  $^1\text{H}$  NMR (DMSO- $d_6$ ):  $\delta_{\text{H}}$  6.33 (s, 2H), 7.00–8.09 (m, 7H).  $^{13}\text{C}$  NMR (DMSO- $d_6$ ):  $\delta_{\text{C}}$  156.6, 153.3, 145.6, 139.1, 137.8, 128.2, 116.8, 115.6, 110.3, 101.9. EI-MS  $m/z$ : 228.26 (M+H) $^+$ . Anal. Calcd for  $\text{C}_{13}\text{H}_{10}\text{FN}_3$ : C, 68.71; H, 4.44; N, 18.49. Found: C, 68.73; H, 4.42; N, 18.47.

#### 4.2.4. General procedure for the synthesis of 4-(5-chloro-1H-benzo[d]imidazol-2-yl)aniline (3c)

The compound was prepared according to the general procedure A using 4-chloro-1,2-phenylenediamine **2c** (1 g, 7.02 mmol), 4-amino benzoic acid (0.96 g, 7.02 mmol) and eatons reagent (10 mL) to afford **3c** (1.1 g, 64% yield) as buff coloured solid. Mp: 291–293 °C.  $^1\text{H}$  NMR (DMSO- $d_6$ ):  $\delta_{\text{H}}$  6.45 (s, 2H), 7.08–8.39 (m, 7H).  $^{13}\text{C}$  NMR (DMSO- $d_6$ ):  $\delta_{\text{C}}$  153.1, 145.7, 133.2, 131.2, 129.6, 128.4, 124.3, 116.7, 116.3, 115.9, 115.2. EI-MS  $m/z$ : 244.42(M+H) $^+$ . Anal. Calcd for  $\text{C}_{13}\text{H}_{10}\text{ClN}_3$ : C, 64.07; H, 4.14; N, 17.24. Found C, 64.11; H, 4.16; N, 17.19.

#### 4.2.5. General procedure for the synthesis of 4-(5-nitro-1H-benzo[d]imidazol-2-yl)aniline (3d)

The compound was prepared according to the general procedure A using 4-nitro-1,2-phenylenediamine **2d** (1 g, 6.53 mmol), 4-amino benzoic acid (0.9 g, 6.53 mmol) and eatons reagent (10 mL) to afford **3d** (1.2 g, 72% yield) as yellowish brown solid. Mp: 277–278 °C.  $^1\text{H}$  NMR (DMSO- $d_6$ ):  $\delta_{\text{H}}$  6.53 (s, 2H), 7.21–8.49 (m, 7H).  $^{13}\text{C}$  NMR (DMSO- $d_6$ ):  $\delta_{\text{C}}$  153.3, 148.6, 145.7, 144.6, 140.2, 128.3, 118.9, 116.3, 116.1, 115.3, 113.2. EI-MS  $m/z$ : 255.44 (M+H) $^+$ . Anal. Calcd for  $\text{C}_{13}\text{H}_{10}\text{N}_4\text{O}_2$ : C, 61.41; H, 3.96 N, 22.04. Found C, 61.44; H, 3.94 N, 22.06.

#### 4.2.6. General procedure for the synthesis of 4-(5-methoxy-1H-benzo[d]imidazol-2-yl)aniline (**3e**)

The compound was prepared according to the general procedure A using 4-methoxy-1,2-phenylenediamine **2e** (1 g, 7.24 mmol), 4-amino benzoic acid (0.99 g, 7.24 mmol) and eatons reagent (10 mL) to afford **3e** (0.91 g, 53%) as reddish brown solid. MP: 162–165 °C. <sup>1</sup>H NMR (DMSO-*d*<sub>6</sub>): δ<sub>H</sub> 3.85 (s, 3H), 6.51 (s, 2H), 7.04–8.13 (m, 7H). <sup>13</sup>C NMR (DMSO-*d*<sub>6</sub>): δ<sub>C</sub> 156.7, 153.4, 145.7, 139.5, 134.5, 128.4, 116.8, 115.3, 112.1, 100.6, 56.1. EI-MS *m/z*: 240.3 (M+H)<sup>+</sup>. Anal. Calcd for C<sub>14</sub>H<sub>13</sub>N<sub>3</sub>O: C, 70.28; H, 5.48; N, 17.56. Found: C, 70.31; H, 5.47; N, 17.58.

#### 4.2.7. General procedure for the synthesis of 4-(3H-imidazo[4,5-b]pyridin-2-yl)aniline (**3f**)

The compound was prepared according to the general procedure A using pyridine-2,3-diamine **2f** (1 g, 9.16 mmol), 4-amino benzoic acid (1.26 g, 9.16 mmol) and eatons reagent (10 mL) to afford **3f** (1.1 g, 58% yield) as pale brown solid. Mp: 265–267 °C. <sup>1</sup>H NMR (DMSO-*d*<sub>6</sub>): δ<sub>H</sub> 6.43 (s, 2H), 7.03–8.22 (m, 7H). <sup>13</sup>C NMR (DMSO-*d*<sub>6</sub>): δ<sub>C</sub> 162.3, 150.7, 145.6, 145.2, 130.5, 128.3, 124.8, 123.6, 122.8, 115.6. EI-MS *m/z*: 211.33 (M+H)<sup>+</sup>. Anal. Calcd for C<sub>12</sub>H<sub>10</sub>N<sub>4</sub>: C, 68.56; H, 4.79; N, 26.65. Found: C, 68.59; H, 4.77; N, 26.62.

#### 4.2.8. General procedure for the synthesis of acylated derivatives (4–6, 8–11, 13–16, 18–21, 23–26, 28–31, 33) procedure B

The synthesis followed the literature procedure. To a well stirred solution of the corresponding 4-(sub:-1H-benzo[d]imidazol-2-yl)aniline/4-(3H-imidazo[4,5-b]pyridin-2-yl)aniline (**3a–f**) (1 equiv) in anhydrous tetrahydrofuran (0.15 M) with 4 Å molecular sieves in an appropriate sized microwave vial; was added the corresponding anhydride (1 equiv) at room temperature. The reaction mixture was then irradiated in Biotage microwave initiator with stirring at 160–170 °C for about 20–30 min (monitored by TLC and LCMS for completion). The solvent was removed under vacuum, diluted with water and basified with solid sodium bicarbonate to a pH of 9. The aqueous layer was further washed with dichloromethane, acidified with 2 N HCl to a pH of 2, and extracted repeatedly with ethyl acetate. The combined organic layer was then dried over anhydrous sodium sulfate and concentrated under reduced pressure. The residue obtained was further recrystallized from ethanol to afford the desired product in good yield and purity as described below.

##### 4.2.9.1. 3-((4-(1H-Benzo[d]imidazol-2-yl)phenyl)amino)-3-oxopropanoic acid (**4**).

The compound was prepared according to the general procedure B using 4-(1H-benzo[d]imidazol-2-yl)aniline **3a** (0.2 g, 0.96 mmol), malonic anhydride (0.082 g, 0.96 mmol) to afford **4** (0.174 g, 61% yield) as pale yellow solid. Mp: 279–281 °C. <sup>1</sup>H NMR (DMSO-*d*<sub>6</sub>): δ<sub>H</sub> 3.25 (s, 2H), 7.44–8.24 (m, 8H), 10.12 (s, 1H), 12.73 (b, 1H). <sup>13</sup>C NMR (DMSO-*d*<sub>6</sub>): δ<sub>C</sub> 172, 163.3, 153.5, 141.5, 139, 128.3, 123.5, 122.2, 120.6, 115.7, 37.3. EI-MS *m/z*: 296.4 (M+H)<sup>+</sup>. Anal. Calcd for C<sub>19</sub>H<sub>13</sub>N<sub>3</sub>O<sub>3</sub>: C, 65.08; H, 4.44; N, 14.23. Found: C, 65.11; H, 4.47; N, 14.28.

##### 4.2.9.2. 4-((4-(1H-Benzo[d]imidazol-2-yl)phenyl)amino)-4-oxobutanoic acid (**5**).

The compound was prepared according to the general procedure B using 4-(1H-benzo[d]imidazol-2-yl)aniline **3a** (0.2 g, 0.96 mmol), succinic anhydride (0.096 g, 0.96 mmol) to afford **5** (0.21 g, 71%) as off white solid. Mp: 259–261 °C. <sup>1</sup>H NMR (DMSO-*d*<sub>6</sub>): δ<sub>H</sub> 2.34–2.91 (m, 4H), 7.42–8.24 (m, 8H), 10.14 (s, 1H), 12.63 (b, 1H). <sup>13</sup>C NMR (DMSO-*d*<sub>6</sub>): δ<sub>C</sub> 177.5, 174.2, 153.4, 141.4, 139, 127.5, 123.5, 122.1, 120.2, 115.8, 30.9, 29.5. EI-MS *m/z*: 310.3 (M+H)<sup>+</sup>. Anal. Calcd for C<sub>17</sub>H<sub>15</sub>N<sub>3</sub>O<sub>3</sub>: C, 66.01; H, 4.89; N, 13.58. Found: C, 66.05; H, 4.84; N, 13.54.

##### 4.2.9.3. 6-((4-(1H-Benzo[d]imidazol-2-yl)phenyl)amino)-6-oxohexanoic acid (**7**).

The compound was prepared according to the general procedure B using 4-(1H-benzo[d]imidazol-2-yl)aniline **3a** (0.2 g, 0.96 mmol), adipic anhydride (0.122 g, 0.96 mmol) to afford **7** (0.211 g, 65% yield) as yellow solid. MP: 276–278 °C. <sup>1</sup>H NMR (DMSO-*d*<sub>6</sub>): δ<sub>H</sub> 1.34–2.42 (m, 8H), 7.48–8.32 (m, 8H), 10.11 (s, 1H), 12.53 (b, 1H). <sup>13</sup>C NMR (DMSO-*d*<sub>6</sub>): δ<sub>C</sub> 180.2, 178.7, 152.7, 142.2, 139.1, 128, 123.3, 122.2, 120.1, 115.8, 37.5, 32.8, 27.9, 24.4. EI-MS *m/z*: 338.2 (M+H)<sup>+</sup>. Anal. Calcd for C<sub>19</sub>H<sub>19</sub>N<sub>3</sub>O<sub>3</sub>: C, 67.64; H, 5.68; N, 12.46. Found: C, 67.61; H, 5.71; N, 12.43.

##### 4.2.9.4. 3-((4-(5-Fluoro-1H-benzo[d]imidazol-2-yl)phenyl)amino)-3-oxopropanoic acid (**8**).

The compound was prepared according to the general procedure B using 4-(5-fluoro-1H-benzo[d]imidazol-2-yl)aniline **3b** (0.2 g, 0.88 mmol), malonic anhydride (0.076 g, 0.88 mmol) to afford **8** (0.188 g, 68% yield) as off white solid. Mp: 210–212 °C. <sup>1</sup>H NMR (DMSO-*d*<sub>6</sub>): δ<sub>H</sub> 1.71–2.39 (m, 2H), 7.03–8.25 (m, 7H) 10.16 (s, 1H), 12.68 (b, 1H). <sup>13</sup>C NMR (DMSO-*d*<sub>6</sub>): δ<sub>C</sub> 172.3, 163.1, 157.2, 153.2, 141.2, 138.7, 137.8, 128.2, 122.3, 120.3, 117.4, 110.3, 102.8, 39.6. EI-MS *m/z*: 314.3 (M+H)<sup>+</sup>. Anal. Calcd for C<sub>16</sub>H<sub>12</sub>FN<sub>3</sub>O<sub>3</sub>: C, 61.34; H, 3.86; N, 13.41. Found: C, 61.38; H, 3.89; N, 13.45.

##### 4.2.9.5. 4-((4-(5-Fluoro-1H-benzo[d]imidazol-2-yl)phenyl)amino)-4-oxobutanoic acid (**9**).

The compound was prepared according to the general procedure B using 4-(5-fluoro-1H-benzo[d]imidazol-2-yl)aniline **3b** (0.2 g, 0.88 mmol), succinic anhydride (0.088 g, 0.88 mmol) to afford **9** (0.193 g, 67% yield) as off white solid. Mp–297–299 °C. <sup>1</sup>H NMR (DMSO-*d*<sub>6</sub>): δ<sub>H</sub> 2.35–2.68 (m, 4H), 7.03–8.29 (m, 7H) 10.14 (s, 1H), 12.65 (b, 1H). <sup>13</sup>C NMR (DMSO-*d*<sub>6</sub>): δ<sub>C</sub> 177.8, 174.2, 156.8, 153.2, 140.8, 138.6, 137.8, 128.3, 122.4, 120.3, 117.4, 110.4, 102.6, 30.5, 28.3. EI-MS *m/z*: 328.42 (M+H). Anal. Calcd for C<sub>17</sub>H<sub>14</sub>FN<sub>3</sub>O<sub>3</sub>: C, 62.38; H, 4.31; N, 12.84. Found: C, 62.35; H, 4.36; N, 12.86.

##### 4.2.9.6. 5-((4-(5-Fluoro-1H-benzo[d]imidazol-2-yl)phenyl)amino)-5-oxopentanoic acid (**10**).

The compound was prepared according to the general procedure B using 4-(5-fluoro-1H-benzo[d]imidazol-2-yl)aniline **3b** (0.2 g, 0.88 mmol), glutaric anhydride (0.1 g, 0.88 mmol) to afford **10** as off white solid. Mp–282–284 °C. <sup>1</sup>H NMR (DMSO-*d*<sub>6</sub>): δ<sub>H</sub> 1.77–2.37 (m, 6H), 7.00–8.08 (m, 7H), 10.16 (s, 1H), 12.91 (b, 1H). <sup>13</sup>C NMR (DMSO-*d*<sub>6</sub>): δ<sub>C</sub> 174.3, 171.2, 160.2, 157, 152.6, 140.9, 124.4, 119.1, 109.76, 35.5, 33.1, 20.4. EI-MS *m/z*: 342.56 (M+H)<sup>+</sup>. Anal. Calcd for C<sub>18</sub>H<sub>16</sub>FN<sub>3</sub>O<sub>3</sub>: C, 63.34; H, 4.72; N, 12.31. Found: C, 63.36; H, 4.71; N, 12.32.

##### 4.2.9.7. 6-((4-(5-Fluoro-1H-benzo[d]imidazol-2-yl)phenyl)amino)-6-oxohexanoic acid (**12**).

The compound was prepared according to the general procedure B using 4-(5-fluoro-1H-benzo[d]imidazol-2-yl)aniline **3b** (0.2 g, 0.88 mmol), adipic anhydride (0.113 g, 0.88 mmol) to afford **12** (0.232 g, 74% yield) as off white solid. Mp–282–284 °C. <sup>1</sup>H NMR (DMSO-*d*<sub>6</sub>): δ<sub>H</sub> 1.35–2.48 (m, 8H), 7.05–8.31 (m, 7H) 10.16 (s, 1H), 12.62 (b, 1H). <sup>13</sup>C NMR (DMSO-*d*<sub>6</sub>): δ<sub>C</sub> 180.2, 178.9, 156.7, 153.4, 140.6, 138.9, 137.5, 128.4, 122.3, 120.2, 117.2, 110.3, 102.5, 38.2, 33.6, 27.5, 24.2. EI-MS *m/z*: 356.4 (M+H)<sup>+</sup>. Anal. Calcd for C<sub>19</sub>H<sub>18</sub>FN<sub>3</sub>O<sub>3</sub>: C, 64.22; H, 5.11; F, 5.35; N, 11.82. Found: C, 64.25; H, 5.16; F, 5.39; N, 11.87.

##### 4.2.9.8. 3-((4-(5-Chloro-1H-benzo[d]imidazol-2-yl)phenyl)amino)-3-oxopropanoic acid (**13**).

The compound was prepared according to the general procedure B using 4-(5-chloro-1H-benzo[d]imidazol-2-yl)aniline **3c** (0.2 g, 0.82 mmol), malonic anhydride (0.071 g, 0.82 mmol) to afford **13** (0.178 g, 66% yield) as pale brown solid. Mp–276–278 °C. <sup>1</sup>H NMR (DMSO-*d*<sub>6</sub>): δ<sub>H</sub> 3.25 (s, 2H), 7.25–8.42 (m, 7H) 10.16 (s, 1H), 12.73 (b, 1H). <sup>13</sup>C NMR (DMSO-*d*<sub>6</sub>): δ<sub>C</sub> 171.8, 163.2, 153.2, 138.7, 133.2, 131.3, 129.4,

128.2, 124.5, 122.3, 120.3, 116.8, 115.9, 39.6. EI-MS  $m/z$ : 330.5 (M+H)<sup>+</sup>. Anal. Calcd for C<sub>16</sub>H<sub>12</sub>ClN<sub>3</sub>O<sub>3</sub>: C, 58.28; H, 3.67 N, 12.74. Found: C, 58.29; H, 3.65 N, 12.77.

**4.2.9.9. 4-((4-(5-Chloro-1H-benzo[d]imidazol-2-yl)phenyl)-amino)-4-oxobutanoic acid (14).** The compound was prepared according to the general procedure B using 4-(5-chloro-1H-benzo[d]imidazol-2-yl)aniline **3c** (0.2 g, 0.82 mmol), succinic anhydride (0.082 g, 0.82 mmol) to afford **14** (0.19 g, 68% yield) as pale brown solid. Mp–288–290 °C. <sup>1</sup>H NMR (DMSO-*d*<sub>6</sub>): δ<sub>H</sub> 2.37–2.68 (s, 4H), 7.23–8.36 (m, 7H) 10.15 (s, 1H), 12.69 (b, 1H). <sup>13</sup>C NMR (DMSO-*d*<sub>6</sub>): δ<sub>C</sub> 177.8, 174.2, 153.3, 138.8, 133.2, 131.3, 129.4, 128.2, 124.5, 122.2, 120.2, 116.7, 155.9, 30.5, 28.8. EI-MS  $m/z$ : 344.6 (M+H)<sup>+</sup>. Anal. Calcd for C<sub>17</sub>H<sub>14</sub>ClN<sub>3</sub>O<sub>3</sub>: C, 59.40; H, 4.10 N, 12.22. Found: C, 59.43; H, 4.12 N, 12.18.

**4.2.9.10. 5-((4-(5-Chloro-1H-benzo[d]imidazol-2-yl)phenyl)-amino)-5-oxopentanoic acid (15).** The compound was prepared according to the general procedure B using 4-(5-chloro-1H-benzo[d]imidazol-2-yl)aniline **3c** (0.2 g, 0.82 mmol), glutaric anhydride (0.094 g, 0.82 mmol) to afford **15** (0.175 g, 59% yield) as off white solid. Mp–274–276 °C. <sup>1</sup>H NMR (DMSO-*d*<sub>6</sub>): δ<sub>H</sub> 1.65–2.28 (m, 6H), 7.23–8.46 (m, 7H) 10.21 (s, 1H), 12.85 (b, 1H). <sup>13</sup>C NMR (DMSO-*d*<sub>6</sub>): δ<sub>C</sub> 180.2, 178.6, 153.2, 138.9, 133.2, 131.2, 129.4, 128.3, 124.5, 122.3, 120.2, 116.8, 115.9, 37.5, 32.8, 20.5. EI-MS  $m/z$ : 358.9 (M+H)<sup>+</sup>. Anal. Calcd for C<sub>18</sub>H<sub>16</sub>ClN<sub>3</sub>O<sub>3</sub>: C, 60.42; H, 4.51; N, 11.74. Found C, 60.44; H, 4.49; N, 11.71.

**4.2.9.11. 6-((4-(5-Chloro-1H-benzo[d]imidazol-2-yl)phenyl)-amino)-6-oxohexanoic acid (17).** The compound was prepared according to the general procedure B using 4-(5-chloro-1H-benzo[d]imidazol-2-yl)aniline **3c** (0.2 g, 0.82 mmol), adipic anhydride (0.105 g, 0.82 mmol) to afford **17** (0.198g, 65% yield) as pale brown solid. Mp–255–257 °C. <sup>1</sup>H NMR (DMSO-*d*<sub>6</sub>): δ<sub>H</sub> 1.46–2.32 (m, 8H), 7.26–8.37 (m, 7H) 10.17 (s, 1H), 12.59 (b, 1H). <sup>13</sup>C NMR (DMSO-*d*<sub>6</sub>): δ<sub>C</sub> 180.2, 178.8, 153.4, 138.7, 134.2, 131.2, 129.5, 128.3, 124.3, 122.3, 120.2, 116.7, 115.9, 38.2, 33.5, 27.3, 24.1. EI-MS  $m/z$ : 372.6 (M+H)<sup>+</sup>. Anal. Calcd for C<sub>19</sub>H<sub>18</sub>ClN<sub>3</sub>O<sub>3</sub>: C, 61.38; H, 4.88 N, 11.30. Found: C, 61.36; H, 4.90 N, 11.31.

**4.2.9.12. 3-((4-(5-Nitro-1H-benzo[d]imidazol-2-yl)phenyl)-amino)-3-oxopropanoic acid (18).** The compound was prepared according to the general procedure B using 4-(5-nitro-1H-benzo[d]imidazol-2-yl)aniline **3d** (0.2 g, 0.79 mmol), malonic anhydride (0.068 g, 0.79 mmol) to afford **18** (0.185 g, 69% yield) as pale yellow solid. Mp–244–246 °C. <sup>1</sup>H NMR (DMSO-*d*<sub>6</sub>): δ<sub>H</sub> 3.21 (s, 2H), 7.71–8.57 (m, 7H), 10.16 (s, 1H), 12.61 (b, 1H). <sup>13</sup>C NMR (DMSO-*d*<sub>6</sub>): δ<sub>C</sub> 171.7, 163.5, 153.2, 148.9, 144.6, 140.2, 138.7, 128.3, 122.2, 120.1, 118.8, 116.3, 113.2, 39.8. EI-MS  $m/z$ : 341.7 (M+H)<sup>+</sup>. Anal. Calcd for C<sub>16</sub>H<sub>12</sub>N<sub>4</sub>O<sub>5</sub>: C, 56.47; H, 3.55; N, 16.46. Found: C, 56.49; H, 3.54; N, 16.48.

**4.2.9.13. 4-((4-(5-Nitro-1H-benzo[d]imidazol-2-yl)phenyl)-amino)-4-oxobutanoic acid (19).** The compound was prepared according to the general procedure B using 4-(5-nitro-1H-benzo[d]imidazol-2-yl)aniline **3d** (0.2 g, 0.79 mmol), succinic anhydride (0.079 g, 0.79 mmol) to afford **19** (0.195 g, 70% yield) as yellow solid. Mp–298–300 °C. <sup>1</sup>H NMR (DMSO-*d*<sub>6</sub>): δ<sub>H</sub> 2.35–2.66 (s, 4H), 7.61–8.49 (m, 7H) 10.15 (s, 1H), 12.69 (b, 1H). <sup>13</sup>C NMR (DMSO-*d*<sub>6</sub>): δ<sub>C</sub> 177.8, 174.2, 153.2, 147.9, 144.5, 140.1, 138.8, 127.8, 122.3, 119.9, 118.7, 116.5, 113.2, 30.5, 28.8. EI-MS  $m/z$ : 355.5 (M+H)<sup>+</sup>. Anal. Calcd for C<sub>17</sub>H<sub>14</sub>N<sub>4</sub>O<sub>5</sub>: C, 57.63; H, 3.98 N, 15.81. Found: C, 57.66; H, 3.97; N, 15.85.

**4.2.9.14. 5-((4-(5-Nitro-1H-benzo[d]imidazol-2-yl)phenyl)-amino)-5-oxopentanoic acid (20).** The compound was

prepared according to the general procedure B using 4-(5-nitro-1H-benzo[d]imidazol-2-yl)aniline **3d** (0.2 g, 0.79 mmol), glutaric anhydride (0.09 g, 0.79 mmol) to afford **20** (0.221 g, 76% yield) as yellow solid. <sup>1</sup>H NMR (DMSO-*d*<sub>6</sub>): δ<sub>H</sub> 1.71–2.36 (m, 6H), 7.73–8.57 (m, 7H), 10.16 (s, 1H), 12.56 (b, 1H). <sup>13</sup>C NMR (DMSO-*d*<sub>6</sub>): δ<sub>C</sub> 180.2, 178.8, 153.4, 148.2, 144.6, 140.2, 138.8, 128.3, 122.2, 120.2, 118.8, 116.3, 133.2, 37.1, 32.5, 20.5. EI-MS  $m/z$ : 369.5 (M+H)<sup>+</sup>. Anal. Calcd for C<sub>18</sub>H<sub>16</sub>N<sub>4</sub>O<sub>5</sub>: C, 58.69; H, 4.38 N, 15.21. Found: C, 58.72; H, 4.37 N, 15.21.

**4.2.9.15. 6-((4-(5-Nitro-1H-benzo[d]imidazol-2-yl)phenyl)-amino)-6-oxohexanoic acid (22).** The compound was prepared according to the general procedure B using 4-(5-nitro-1H-benzo[d]imidazol-2-yl)aniline **3d** (0.2 g, 0.79 mmol), adipic anhydride (0.1 g, 0.79 mmol) to afford **22** (0.21 g, 66% yield) as yellow solid. Mp–298–300 °C. <sup>1</sup>H NMR (DMSO-*d*<sub>6</sub>): δ<sub>H</sub> 1.42–2.34 (m, 8H), 7.67–8.58 (m, 7H), 10.16 (s, 1H), 12.65 (b, 1H). <sup>13</sup>C NMR (DMSO-*d*<sub>6</sub>): δ<sub>C</sub> 180.1, 178.6, 153.1, 148.2, 144.5, 140.1, 138.8, 128.3, 122.2, 120.2, 118.8, 116.2, 113.2, 38.2, 33.6, 27.2, 23.9. EI-MS  $m/z$ : 383.3 (M+H)<sup>+</sup>. Anal. Calcd for C<sub>19</sub>H<sub>18</sub>N<sub>4</sub>O<sub>5</sub>: C, 59.68; H, 4.74; N, 14.65. Found: C, 59.66; H, 4.77; N, 14.68.

**4.2.9.16. 3-((4-(5-Methoxy-1H-benzo[d]imidazol-2-yl)phenyl)-amino)-3-oxopropanoic acid (23).** The compound was prepared according to the general procedure B using 4-(5-methoxy-1H-benzo[d]imidazol-2-yl)aniline **3e** (0.2 g, 0.84 mmol), malonic anhydride (0.072 g, 0.84 mmol) to afford **23** (0.183 g, 67% yield) as yellow solid. Mp–277–279 °C. <sup>1</sup>H NMR (DMSO-*d*<sub>6</sub>): δ<sub>H</sub> 3.36 (s, 2H), 3.89 (s, 3H), 7.06–8.31 (m, 7H) 10.12 (s, 1H), 12.55 (b, 1H). <sup>13</sup>C NMR (DMSO-*d*<sub>6</sub>): δ<sub>C</sub> 172.5, 162.5, 156.4, 153.2, 140.1, 138.2, 133.8, 127.3, 122.3, 120.1, 115.8, 112.5, 101.2, 56.5, 40.2. EI-MS  $m/z$ : 326.4 (M+H)<sup>+</sup>. Anal. Calcd for C<sub>17</sub>H<sub>15</sub>N<sub>3</sub>O<sub>4</sub>: C, 62.76; H, 4.65; N, 12.92. Found: C, 62.74; H, 4.68; N, 12.89.

**4.2.9.17. 4-((4-(5-Methoxy-1H-benzo[d]imidazol-2-yl)phenyl)-amino)-4-oxobutanoic acid (24).** The compound was prepared according to the general procedure B using 4-(5-methoxy-1H-benzo[d]imidazol-2-yl)aniline **3e** (0.2 g, 0.84 mmol), succinic anhydride (0.084 g, 0.84 mmol) to afford **24** (0.169 g, 60% yield) as pale brown solid. Mp–180–182 °C. <sup>1</sup>H NMR (DMSO-*d*<sub>6</sub>): δ<sub>H</sub> 2.36–2.62 (m, 4H), 3.87 (s, 3H), 7.02–8.33 (m, 7H) 10.13 (s, 1H), 12.61 (b, 1H). <sup>13</sup>C NMR (DMSO-*d*<sub>6</sub>): δ<sub>C</sub> 177.8, 174.3, 156.5, 153.2, 140.3, 138.7, 134.2, 128.3, 122.3, 120.2, 116.7, 112.2, 100.9, 56.5, 30.7, 28.8. EI-MS  $m/z$ : 340.45 (M+H)<sup>+</sup>. Anal. Calcd for C<sub>18</sub>H<sub>17</sub>N<sub>3</sub>O<sub>4</sub>: C, 63.71; H, 5.05; N, 12.38. Found: C, 63.75; H, 5.01; N, 12.40.

**4.2.9.18. 5-((4-(5-Methoxy-1H-benzo[d]imidazol-2-yl)phenyl)-amino)-5-oxopentanoic acid (25).** The compound was prepared according to the general procedure B using 4-(5-nitro-1H-benzo[d]imidazol-2-yl)aniline **3e** (0.2 g, 0.84 mmol), glutaric anhydride (0.095 g, 0.84 mmol) to afford **25** (0.186 g, 63% yield) as brown solid. Mp–212–214 °C. <sup>1</sup>H NMR (DMSO-*d*<sub>6</sub>): δ<sub>H</sub> 1.66–2.33 (m, 6H), 3.94 (s, 3H), 7.05–8.26 (m, 7H) 10.11 (s, 1H), 12.73 (b, 1H). <sup>13</sup>C NMR (DMSO-*d*<sub>6</sub>): δ<sub>C</sub> 180.3, 177.6, 156.5, 153.6, 139.2, 138.5, 134.4, 128.7, 122.3, 120.5, 116.8, 112.3, 100.9, 56.5, 37.2, 33.2, 20.9. EI-MS  $m/z$ : 354.4 (M+H)<sup>+</sup>. Anal. Calcd for C<sub>19</sub>H<sub>19</sub>N<sub>3</sub>O<sub>4</sub>: C, 64.58; H, 5.42; N, 11.89. Found: C, 64.54; H, 5.45; N, 11.91.

**4.2.9.19. 6-((4-(5-Methoxy-1H-benzo[d]imidazol-2-yl)phenyl)-amino)-6-oxohexanoic acid (27).** The compound was prepared according to the general procedure B using 4-(5-methoxy-1H-benzo[d]imidazol-2-yl)aniline **3e** (0.2 g, 0.84 mmol), adipic anhydride (0.107 g, 0.84 mmol) to afford **27** (0.218 g, 71% yield) as reddish brown solid. Mp–171–173 °C. <sup>1</sup>H NMR

(DMSO- $d_6$ ):  $\delta_H$  1.39–2.35 (m, 8H), 3.86 (s, 3H), 7.04–8.26 (m, 7H) 10.16 (s, 1H), 12.66 (b, 1H).  $^{13}C$  NMR (DMSO- $d_6$ ):  $\delta_C$  180.2, 178.5, 156.7, 153.2, 140.2, 138.7, 133.8, 128.3, 121.7, 120.3, 116.7, 112.2, 100.6, 56.2, 38.2, 33.5, 27.6, 24.5. EI-MS  $m/z$ : 368.5 (M+H) $^+$ . Anal. Calcd for  $C_{20}H_{21}N_3O_4$ : C, 65.38; H, 5.76; N, 11.44. Found: C, 65.35; H, 5.78; N, 11.46.

**4.2.9.20. 3-((4-(1H-Imidazo[4,5-b]pyridin-2-yl)phenyl)amino)-3-oxopropanoic acid (28).** The compound was prepared according to the general procedure B using 4-(3H-imidazo[4,5-b]pyridin-2-yl)aniline **3e** (0.2 g, 0.95 mmol), malonic anhydride (0.082 g, 0.95 mmol) to afford **28** (0.193 g, 68% yield) as buff coloured solid. Mp–288–290 °C.  $^1H$  NMR (DMSO- $d_6$ ):  $\delta_H$  3.36 (s, 2H), 7.01–8.25 (m, 7H) 10.19 (s, 1H), 12.71 (b, 1H).  $^{13}C$  NMR (DMSO- $d_6$ ):  $\delta_C$  172.3, 163.1, 161.9, 150.8, 145.6, 138.6, 130.3, 128.2, 123.7, 122.8, 120.3, 39.8. EI-MS  $m/z$ : 297.5 (M+H) $^+$ . Anal. Calcd for  $C_{15}H_{12}N_4O_3$ : C, 60.81; H, 4.08; N, 18.91. Found C, 60.85; H, 4.04; N, 18.90.

**4.2.9.21. 4-((4-(1H-Imidazo[4,5-b]pyridin-2-yl)phenyl)amino)-4-oxobutanoic acid (29).** The compound was prepared according to the general procedure B using 4-(3H-imidazo[4,5-b]pyridin-2-yl)aniline **3e** (0.2 g, 0.95 mmol), succinic anhydride (0.095 g, 0.95 mmol) to afford **29** (0.211 g, 71% yield) as off white solid. Mp–233–235 °C.  $^1H$  NMR (DMSO- $d_6$ ):  $\delta_H$  2.36–2.68 (s, 4H), 7.05–8.32 (m, 7H) 10.15 (s, 1H), 12.68 (b, 1H).  $^{13}C$  NMR (DMSO- $d_6$ ):  $\delta_C$  177.8, 174.2, 161.7, 150.6, 145.3, 138.6, 130.6, 128.1, 123.8, 122.6, 120.1, 30.2, 28.6. EI-MS  $m/z$ : 311.3 (M+H) $^+$ . Anal. Calcd for  $C_{16}H_{14}N_4O_3$ : C, 61.93; H, 4.55; N, 18.06. Found: C, 61.95; H, 4.58; N, 18.01.

**4.2.9.22. 5-((4-(1H-Imidazo[4,5-b]pyridin-2-yl)phenyl)amino)-5-oxopentanoic acid (30).** The compound was prepared according to the general procedure B using 4-(3H-imidazo[4,5-b]pyridin-2-yl)aniline **3e** (0.2 g, 0.95 mmol), glutaric anhydride (0.108 g, 0.95 mmol) to afford **30** (0.191 g, 62% yield) as pale brown solid. Mp–271–273 °C.  $^1H$  NMR (DMSO- $d_6$ ):  $\delta_H$  1.71–2.39 (m, 6H), 7.03–8.25 (m, 7H) 10.16 (s, 1H), 12.6 (b, 1H).  $^{13}C$  NMR (DMSO- $d_6$ ):  $\delta_C$  180.1, 178.5, 161.8, 150.6, 145.8, 138.7, 130.5, 128.2, 123.8, 122.7, 120.3, 37.5, 32.5, 20.4. EI-MS  $m/z$ : 325.5 (M+H) $^+$ . Anal. Calcd for  $C_{17}H_{16}N_4O_3$ : C, 62.95; H, 4.97; N, 17.27. Found: C, 62.98; H, 4.96; N, 17.26.

**4.2.9.23. 6-((4-(1H-Imidazo[4,5-b]pyridin-2-yl)phenyl)amino)-6-oxohexanoic acid (32).** The compound was prepared according to the general procedure B using 4-(3H-imidazo[4,5-b]pyridin-2-yl)aniline **3e** (0.2 g, 0.95 mmol), adipic anhydride (0.122 g, 0.95 mmol) to afford **32** (0.22 g, 69% yield) as buff coloured solid. Mp–259–261 °C.  $^1H$  NMR (DMSO- $d_6$ ):  $\delta_H$  1.42–2.32 (m, 8H), 7.03–8.30 (m, 7H) 10.16 (s, 1H), 12.65 (b, 1H).  $^{13}C$  NMR (DMSO- $d_6$ ):  $\delta_C$  180.2, 178.7, 161.8, 150.6, 145.3, 138.9, 130.6, 128.2, 123.6, 122.8, 120.2, 38.2, 33.8, 27.5, 23.9. EI-MS  $m/z$ : 339.5 (M+H) $^+$ . Anal. Calcd for  $C_{18}H_{18}N_4O_3$ : C, 63.89; H, 5.36; N, 16.56. Found: C, 63.92; H, 5.34; N, 16.57.

#### 4.2.10. General procedure for the synthesis of ester derivatives (6, 11, 16, 21, 26, and 31), procedure C

To a well stirred solution of the corresponding carboxylic acid analogues (**1**, **10**, **20**, **25** and **30**) in methanol at 0 °C was added catalytic amount of  $H_2SO_4$ . The reaction was then heated to reflux for about 5–6 h (monitored by TLC and LCMS for completion). The solvent was removed under vacuum, diluted with water and neutralised with 10% sodium bicarbonate solution to a pH of 7, and extracted repeatedly with ethyl acetate, (any trace amount of acid, if left over was removed by sodium bicarbonate washings) The combined organic layer was then dried over anhydrous sodium

sulfate and concentrated under reduced pressure to afford the desired product in good yield and purity as described below.

**4.2.10.1. Methyl 5-((4-(1H-benzo[d]imidazol-2-yl)phenyl)amino)-5-oxopentanoate (6).** The compound was prepared according to the general procedure C using 5-((4-(1H-benzo[d]imidazol-2-yl)phenyl)amino)-5-oxopentanoic acid **1** (0.1 g, 0.31 mmol), to afford **6** (0.23 g, 69% yield) as pale brown solid. Mp–218–220 °C.  $^1H$  NMR (DMSO- $d_6$ ):  $\delta_H$  3.82 (s, 3H), 1.77–2.37 (m, 6H), 7.25–8.21 (m, 8H), 10.14 (s, 1H).  $^{13}C$  NMR (DMSO- $d_6$ ):  $\delta_C$  173.8, 153.1, 141.6, 139.5, 128.5, 123.8, 121.6, 120.2, 115.8, 52.3, 33.2, 20.5. EI-MS  $m/z$ : 338.45 (M+H) $^+$ . Anal. Calcd for  $C_{19}H_{19}N_3O_3$ : C, 67.64; H, 5.68; N, 12.46. Found: C, 67.62; H, 5.72; N, 12.45.

**4.2.10.2. Methyl 5-((4-(5-fluoro-1H-benzo[d]imidazol-2-yl)phenyl)amino)-5-oxopentanoate (11).** The compound was prepared according to the general procedure C using 5-((4-(5-fluoro-1H-benzo[d]imidazol-2-yl)phenyl)amino)-5-oxopentanoic acid **10** (0.1 g, 0.29 mmol), to afford **11** (0.2 g, 63% yield) as off white solid. Mp–244–246 °C.  $^1H$  NMR (DMSO- $d_6$ ):  $\delta_H$  1.61–2.31 (m, 6H), 3.75 (s, 3H), 7.06–8.28 (m, 7H) 10.18 (s, 1H).  $^{13}C$  NMR (DMSO- $d_6$ ):  $\delta_C$  180.2, 173.5, 156.8, 153.2, 140.9, 138.8, 137.6, 128.3, 122.2, 119.6, 117.1, 110.3, 102.2, 52.3, 36.5, 33.1, 20.8. EI-MS  $m/z$ : 356.5 (M+H) $^+$ . Anal. Calcd for  $C_{19}H_{18}FN_3O_3$ : C, 64.22; H, 5.11; N, 11.82. Found: C, 64.28; H, 5.07; N, 11.80.

**4.2.10.3. Methyl 5-((4-(5-chloro-1H-benzo[d]imidazol-2-yl)phenyl)amino)-5-oxopentanoate (16).** The compound was prepared according to the general procedure C using 5-((4-(5-chloro-1H-benzo[d]imidazol-2-yl)phenyl)amino)-5-oxopentanoic acid **15** (0.1 g, 0.28 mmol), to afford **16** (0.21 g, 68% yield) as off white solid. Mp–263–265 °C.  $^1H$  NMR (DMSO- $d_6$ ):  $\delta_H$  1.82–2.32 (m, 6H), 3.85 (s, 3H), 7.21–8.43 (m, 7H) 10.19 (s, 1H).  $^{13}C$  NMR (DMSO- $d_6$ ):  $\delta_C$  180.3, 173.3, 153.4, 138.7, 133.2, 131.2, 129.6, 128.4, 124.3, 122.4, 120.3, 116.7, 115.9, 52.3, 37.3, 32.7, 20.8. EI-MS  $m/z$ : 372.4 (M+H) $^+$ . Anal. Calcd for  $C_{19}H_{18}ClN_3O_3$ : C, 61.38; H, 4.88; N, 11.30. Found C, 61.42; H, 4.85; N, 11.29.

**4.2.10.4. Methyl 5-((4-(5-nitro-1H-benzo[d]imidazol-2-yl)phenyl)amino)-5-oxopentanoate (21).** The compound was prepared according to the general procedure C using 5-((4-(5-nitro-1H-benzo[d]imidazol-2-yl)phenyl)amino)-5-oxopentanoic acid **20** (0.1 g, 0.27 mmol), to afford **21** (0.218 g, 73% yield) as yellow solid. The compound was prepared according to the general procedure C using 5-((4-(5-nitro-1H-benzo[d]imidazol-2-yl)phenyl)amino)-5-oxopentanoic acid **20** (0.1g, mmol), to afford **21** (0.218 g, 73% yield) as yellow solid. Mp–275–277 °C.  $^1H$  NMR (DMSO- $d_6$ ):  $\delta_H$  1.63–2.35 (m, 6H), 3.8 3(s, 3H), 7.69–8.57 (m, 7H) 10.19 (s, 1H).  $^{13}C$  NMR (DMSO- $d_6$ ):  $\delta_C$  180.2, 173.3, 153.3, 148.6, 144.6, 140.2, 138.7, 128.3, 122.3, 120.2, 118.9, 116.3, 113.2, 52.3, 37.5, 32.8, 20.8. EI-MS  $m/z$ : 383.4 (M+H) $^+$ . Anal. Calcd for  $C_{19}H_{18}N_4O_5$ : C, 59.68; H, 4.74 N, 14.65. Found: C, 59.69; H, 4.77 N, 14.62.

**4.2.10.5. Methyl 5-((4-(5-methoxy-1H-benzo[d]imidazol-2-yl)phenyl)amino)-5-oxopentanoate (26).** The compound was prepared according to the general procedure C using 5-((4-(5-methoxy-1H-benzo[d]imidazol-2-yl)phenyl)amino)-5-oxopentanoic acid **25** (0.1 g, 0.28 mmol), to afford **26** (0.188 g, 61% yield) as brown solid. Mp–251–253 °C.  $^1H$  NMR (DMSO- $d_6$ ):  $\delta_H$  1.74–2.35 (m, 6H), 3.72 (s, 3H), 3.95 (s, 3H), 7.02–8.21 (m, 7H) 10.16 (s, 1H).  $^{13}C$  NMR (DMSO- $d_6$ ):  $\delta_C$  180.1, 156.7, 153.4, 139.5, 138.6, 134.5, 128.4, 122.3, 120.2, 116.8, 112.1, 100.6, 56.3, 51.5, 37.1, 33.3, 21.2. EI-MS  $m/z$ : 368.3 (M+H) $^+$ . Anal. Calcd for  $C_{20}H_{21}N_3O_4$ : C, 65.38; H, 5.76; N, 11.44. Found: C, 65.42; H, 5.72; N, 11.46.

**4.2.10.6. Methyl 5-((4-(3H-imidazo[4,5-b]pyridin-2-yl)phenyl)amino)-5-oxopentanoate (31).** The compound was prepared according to the general procedure C using 5-((4-(3H-imidazo[4,5-b]pyridin-2-yl)phenyl)amino)-5-oxopentanoic acid **30** (0.1 g, 0.31 mmol), to afford **31** (0.23 g, 72% yield) as pale brown solid. Mp–230–232 °C. <sup>1</sup>H NMR (DMSO-*d*<sub>6</sub>): δ<sub>H</sub> 1.69–2.32 (m, 6H), 3.43 (s, 3H), 7.03–8.26 (m, 7H) 10.14 (s, 1H). <sup>13</sup>C NMR (DMSO-*d*<sub>6</sub>): δ<sub>C</sub> 180.3, 173.8, 162.3, 150.7, 145.6, 138.7, 130.5, 128.3, 123.9, 122.8, 120.3, 52.4, 37.3, 32.8, 20.8. EI-MS *m/z*: 339.3 (M+H)<sup>+</sup>. Anal. Calcd for C<sub>18</sub>H<sub>18</sub>N<sub>4</sub>O<sub>3</sub>: C, 63.89; H, 5.36; N, 16.56; O, 14.19. Found: C, 63.86; H, 5.39; N, 16.54.

**4.2.11. General procedure for the synthesis of oxygen and thio-substituted acyl derivatives (33–44), procedure D**

To a well stirred solution of the corresponding 4-(sub-1H-benzo[d]imidazol-2-yl)aniline/4-(3H-imidazo[4,5-b]pyridin-2-yl)aniline (**3a–f**) (1 equiv) and triethylamine (2.5 equiv) in dichloromethane was added the appropriate dicarboxylic acid (1 equiv) followed by propylphosphonic anhydride solution (2.5 equiv; 50% solution in ethyl acetate) at 0 °C. The reaction mixture was warmed to room temperature and stirred at room temperature for 8h (monitored by TLC and LCMS for completion). The reaction mixture was then washed with water, brine dried over anhydrous sodium sulfate and concentrated under reduced pressure. The residue obtained was then purified by flash chromatography to afford the desired product in good yield and purity as described below.

**4.2.11.1. 2-(2-((4-(1H-Benzo[d]imidazol-2-yl)phenyl)amino)-2-oxoethoxy)acetic acid (33).** The compound was prepared according to the general procedure D using 4-(1H-benzo[d]imidazol-2-yl)aniline **3a** (0.1 g, 0.48 mmol), triethylamine (0.121 g, 1.2 mmol), 2,2'-oxydiacetic acid (0.064 g, 0.048 mmol) and propylphosphonic anhydride solution (0.38 g, 1.2 mmol) to afford **33** (0.188 g, 61% yield) as off white solid. Mp–244–246 °C. <sup>1</sup>H NMR (DMSO-*d*<sub>6</sub>): δ<sub>H</sub> 4.25 (m, 4H), 7.32–8.14 (m, 8H), 10.16 (s, 1H), 12.83 (b, 1H). <sup>13</sup>C NMR (DMSO-*d*<sub>6</sub>): δ<sub>C</sub> 173.2, 170.1, 153.3, 141.5, 139.2, 127.6, 123.3, 122.2, 120.2, 115.5, 69.2, 68.6. EI-MS *m/z*: 326.4 (M+H)<sup>+</sup>. Anal. Calcd for C<sub>17</sub>H<sub>15</sub>N<sub>3</sub>O<sub>4</sub>: C, 62.76; H, 4.65; N, 12.92. Found: C, 62.79; H, 4.64; N, 12.91.

**4.2.11.2. 2-((2-((4-(1H-Benzo[d]imidazol-2-yl)phenyl)amino)-2-oxoethyl)thio)acetic acid (34).** The compound was prepared according to the general procedure D using 4-(1H-benzo[d]imidazol-2-yl)aniline **3a** (0.1 g, 0.48 mmol), triethylamine (0.121 g, 1.2 mmol), 2,2'-thiodiacetic acid (0.072 g, 0.048 mmol) and propylphosphonic anhydride solution (0.38 g, 1.2 mmol) to afford **34** (0.231 g, 70% yield) as pale brown solid. Mp–184–186 °C. <sup>1</sup>H NMR (DMSO-*d*<sub>6</sub>): δ<sub>H</sub> 3.22 (s, 2H), 3.6 (s, 2H), 7.54–8.34 (m, 8H), 10.15 (s, 1H), 12.93 (b, 1H). <sup>13</sup>C NMR (DMSO-*d*<sub>6</sub>): δ<sub>C</sub> 175.2, 169.1, 153.2, 141.5, 139, 128.1, 123.2, 121.6, 119.5, 115.7, 44, 42.2. EI-MS *m/z*: 342.3 (M+H)<sup>+</sup>. Anal. Calcd for C<sub>17</sub>H<sub>15</sub>N<sub>3</sub>O<sub>3</sub>S: C, 59.81; H, 4.43; N, 12.31. Found: C, 59.78; H, 4.45.

**4.2.11.3. 2-(2-((4-(5-Fluoro-1H-benzo[d]imidazol-2-yl)phenyl)amino)-2-oxoethoxy)acetic acid (35).** The compound was prepared according to the general procedure D using 4-(5-fluoro-1H-benzo[d]imidazol-2-yl)aniline **3b** (0.1 g, 0.44 mmol), triethylamine (0.111 g, 1.1 mmol), 2,2'-oxydiacetic acid (0.059 g, 0.44 mmol) and propylphosphonic anhydride solution (0.35 g, 1.1 mmol) to afford **35** (0.186 g, 62% yield) as pale brown solid. Mp–247–249 °C. <sup>1</sup>H NMR (DMSO-*d*<sub>6</sub>): δ<sub>H</sub> 4.23 (s, 4H), 7.00–8.11 (m, 7H) 10.15 (s, 1H), 12.94 (b, 1H). <sup>13</sup>C NMR (DMSO-*d*<sub>6</sub>): δ<sub>C</sub> 173.3, 170.2, 153.3, 141.1, 139.1, 137.8, 128.2, 122.3, 119.5, 117.2, 110.3, 101.9, 69.2, 68.5. EI-MS *m/z*: 344.02 (M+H)<sup>+</sup>. Anal. Calcd for C<sub>17</sub>H<sub>14</sub>FN<sub>3</sub>O<sub>4</sub>: C, 59.47; H, 4.11; N, 12.24. Found: C, 59.50; H, 4.10; N, 12.25.

**4.2.11.4. 2-((2-((4-(5-Fluoro-1H-benzo[d]imidazol-2-yl)phenyl)amino)-2-oxoethyl)thio)acetic acid (36).** The compound was prepared according to the general procedure D using 4-(5-fluoro-1H-benzo[d]imidazol-2-yl)aniline **3b** (0.1 g, 0.44 mmol), triethylamine (0.111 g, 1.1 mmol), 2,2'-thiodiacetic acid (0.066 g, 0.44 mmol) and propylphosphonic anhydride solution (0.35 g, 1.1 mmol) to afford **36** (0.203 g, 64% yield) as pale brown solid. Mp–159–161 °C. <sup>1</sup>H NMR (DMSO-*d*<sub>6</sub>): δ<sub>H</sub> 3.2 (s, 2H), 3.41 (s, 2H), 7.06–8.33 (m, 7H) 10.18 (s, 1H), 12.59 (b, 1H). <sup>13</sup>C NMR (DMSO-*d*<sub>6</sub>): δ<sub>C</sub> 175.1, 168.8, 156.8, 153.2, 140.7, 139.1, 137.5, 128.4, 122.3, 120.2, 117.3, 110.3, 102.8, 44.1, 41.7. EI-MS *m/z*: 360.6 (M+H)<sup>+</sup>. Anal. Calcd for C<sub>17</sub>H<sub>14</sub>FN<sub>3</sub>O<sub>3</sub>S: C, 56.82; H, 3.93; N, 11.69. Found: C, 56.85; H, 3.89; N, 11.71.

**4.2.11.5. 2-(2-((4-(5-Chloro-1H-benzo[d]imidazol-2-yl)phenyl)amino)-2-oxoethoxy)acetic acid (37).** The compound was prepared according to the general procedure D using 4-(5-chloro-1H-benzo[d]imidazol-2-yl)aniline **3c** (0.1 g, 0.41 mmol), triethylamine (0.104 g, 1.03 mmol), 2,2'-oxydiacetic acid (0.055 g, 0.41 mmol) and propylphosphonic anhydride solution (0.326 g, 1.03 mmol) to afford **37** (0.207 g, 70% yield) as off white solid. Mp–278–280 °C. <sup>1</sup>H NMR (DMSO-*d*<sub>6</sub>): δ<sub>H</sub> 4.26 (s, 4H), 7.26–8.48 (m, 7H) 10.11 (s, 1H), 12.8 (b, 1H). <sup>13</sup>C NMR (DMSO-*d*<sub>6</sub>): δ<sub>C</sub> 173.2, 169.5, 153.4, 138.8, 133.1, 131.5, 129.5, 127.9, 124.5, 122.2, 120.2, 116.8, 115.9, 69.3, 67.8. EI-MS *m/z*: 360.7 (M+H)<sup>+</sup>. Anal. Calcd for C<sub>17</sub>H<sub>14</sub>ClN<sub>3</sub>O<sub>4</sub>: C, 56.75; H, 3.92; N, 11.68. Found C, 56.79; H, 3.88; N, 11.69.

**4.2.11.6. 2-((2-((4-(5-Chloro-1H-benzo[d]imidazol-2-yl)phenyl)amino)-2-oxoethyl)thio)acetic acid (38).** The compound was prepared according to the general procedure D using 4-(5-chloro-1H-benzo[d]imidazol-2-yl)aniline **3c** (0.1 g, 0.41 mmol), triethylamine (0.104 g, 1.03 mmol), 2,2'-thiodiacetic acid (0.062 g, 0.41 mmol) and propylphosphonic anhydride solution (g, 1.03 mmol) to afford **38** (0.227 g, 74% yield) as off white solid. Mp–278–280 °C. <sup>1</sup>H NMR (DMSO-*d*<sub>6</sub>): δ<sub>H</sub> 3.21 (s, 2H), 3.40 (s, 2H), 7.24–8.39 (m, 7H) 10.18 (s, 1H), 12.65 (b, 1H). <sup>13</sup>C NMR (DMSO-*d*<sub>6</sub>): δ<sub>C</sub> 174.8, 168.6, 153.2, 138.7, 133.2, 131.2, 129.4, 128.2, 124.5, 122.2, 120.3, 116.8, 115.9, 43.8, 41.4. EI-MS *m/z*: 376.3 (M+H)<sup>+</sup>. Anal. Calcd for C<sub>17</sub>H<sub>14</sub>ClN<sub>3</sub>O<sub>3</sub>S: C, 54.33; H, 3.75; N, 11.18. Found: C, 54.35; H, 3.77; N, 11.14.

**4.2.11.7. 2-(2-((4-(5-Nitro-1H-benzo[d]imidazol-2-yl)phenyl)amino)-2-oxoethoxy)acetic acid (39).** The compound was prepared according to the general procedure D using 4-(5-chloro-1H-benzo[d]imidazol-2-yl)aniline **3d** (0.1 g, 0.39 mmol), triethylamine, (0.1 g, 0.98 mmol), 2,2'-oxydiacetic acid (0.053 g, 0.39 mmol) and propylphosphonic anhydride solution (0.313 g, 0.98 mmol) to afford **39** (0.173 g, 59% yield) as yellow solid. Mp–251–253 °C. <sup>1</sup>H NMR (DMSO-*d*<sub>6</sub>): δ<sub>H</sub> 4.23 (s, 4H), 7.72–8.55 (m, 7H), 10.15 (s, 1H), 12.58 (b, 1H). <sup>13</sup>C NMR (DMSO-*d*<sub>6</sub>): δ<sub>C</sub> 173.2, 169.8, 153.2, 147.9, 144.6, 140.2, 138.1, 122.2, 128.3, 119.9, 118.7, 116.5, 113.2, 69.2, 68.2. EI-MS *m/z*: 371.3 (M+H)<sup>+</sup>. Anal. Calcd for C<sub>17</sub>H<sub>14</sub>N<sub>4</sub>O<sub>6</sub>: C, 55.14; H, 3.81; N, 15.13. Found: C, 55.16; H, 3.79; N, 15.12.

**4.2.11.8. 2-((2-((4-(5-Nitro-1H-benzo[d]imidazol-2-yl)phenyl)amino)-2-oxoethyl)thio)acetic acid (40).** The compound was prepared according to the general procedure D using 4-(5-chloro-1H-benzo[d]imidazol-2-yl)aniline **3d** (0.1 g, 0.39 mmol), triethylamine (0.1 g, 0.98 mmol) and propylphosphonic anhydride solution (0.313 g, 0.98 mmol) to afford **40** (0.173 g, 57% yield) as yellow solid. Mp–231–233 °C. <sup>1</sup>H NMR (DMSO-*d*<sub>6</sub>): δ<sub>H</sub> 3.25 (s, 2H), 3.39 (s, 2H), 7.69–8.52 (m, 7H), 10.14 (s, 1H), 12.68 (b, 1H). <sup>13</sup>C NMR (DMSO-*d*<sub>6</sub>): δ<sub>C</sub> 174.8, 168.5, 153.2, 148.2, 144.5, 140.1, 138.8, 128.1,

122.3, 120.2, 118.7, 116.5, 113.3, 43.8, 41.5. EI-MS  $m/z$ : 387.6 (M+H)<sup>+</sup>. Anal. Calcd for C<sub>17</sub>H<sub>14</sub>N<sub>4</sub>O<sub>5</sub>S: C, 52.84; H, 3.65; N, 14.50. Found C, 52.86; H, 3.63; N, 14.52.

**4.2.11.9. 2-(2-((4-(5-Methoxy-1H-benzo[d]imidazol-2-yl)phenyl)amino)-2-oxoethoxy)acetic acid (41).** The compound was prepared according to the general procedure D using 4-(5-methoxy-1H-benzo[d]imidazol-2-yl)aniline **3e** (0.1 g, 0.42 mmol), triethylamine (0.11 g, 1.05 mmol), 2,2'-oxydiacetic acid (0.056 g, 0.42 mmol) and propylphosphonic anhydride solution (0.332 g, 1.05 mmol) to afford **41** (0.208 g, 70% yield) as buff coloured solid. Mp–234–236 °C. <sup>1</sup>H NMR (DMSO-*d*<sub>6</sub>): δ<sub>H</sub> 4.26 (s, 4H), 3.91 (s, 3H), 7.03–8.24 (m, 7H) 10.15 (s, 1H), 12.65 (b, 1H). <sup>13</sup>C NMR (DMSO-*d*<sub>6</sub>): δ<sub>C</sub> 171.3, 165.8, 155.8, 153.2, 139.8, 138.2, 134.8, 128.3, 122.3, 119.8, 115.8, 112.2, 100.3, 68.5, 56.8. EI-MS  $m/z$ : 356.3 (M+H)<sup>+</sup>. Anal. Calcd for C<sub>18</sub>H<sub>17</sub>N<sub>3</sub>O<sub>5</sub>S: C, 60.84; H, 4.82; N, 11.83. Found: C, 60.87; H, 4.79; N, 11.85.

**4.2.11.10. 2-(2-((4-(5-Methoxy-1H-benzo[d]imidazol-2-yl)phenyl)amino)-2-oxoethyl)thio)acetic acid (42).** The compound was prepared according to the general procedure D using 4-(5-methoxy-1H-benzo[d]imidazol-2-yl)aniline **3e** (0.1 g, 0.42 mmol), triethylamine (0.11 g, 1.05 mmol), 2,2'-thiodiacetic acid (0.063 g, 0.42 mmol) and propylphosphonic anhydride solution (0.332 g, 1.05 mmol) to afford **42** (0.189 g, 61% yield) as dark brown solid. Mp–250–252 °C. <sup>1</sup>H NMR (DMSO-*d*<sub>6</sub>): δ<sub>H</sub> 3.26 (s, 2H), 3.39 (s, 2H), 3.92 (s, 3 H), 7.09–8.29 (m, 7H) 10.11 (s, 1H), 12.81 (b, 1H). <sup>13</sup>C NMR (DMSO-*d*<sub>6</sub>): δ<sub>C</sub> 174.8, 169.1, 156.7, 153.1, 140.2, 138.7, 133.9, 128.2, 122.3, 120.2, 115.9, 111.8, 101.3, 56.3, 44.2, 41.8. EI-MS  $m/z$ : 372.5 (M+H)<sup>+</sup>. Anal. Calcd for C<sub>18</sub>H<sub>17</sub>N<sub>3</sub>O<sub>4</sub>S: C, 58.21; H, 4.61; N, 11.31. Found: C, 58.25; H, 4.65; N, 11.30.

**4.2.11.11. 2-(2-((4-(3H-Imidazo[4,5-*b*]pyridin-2-yl)phenyl)amino)-2-oxoethoxy)acetic acid (43).** The compound was prepared according to the general procedure D using 4-(3H-imidazo[4,5-*b*]pyridin-2-yl)aniline **3f** (0.1 g, 0.48 mmol), triethylamine, acid (0.12 g, 1.2 mmol), 2,2'-oxydiacetic acid (0.063 g, 0.48 mmol) and propylphosphonic anhydride solution (0.38 g, 1.2 mmol) to afford **43** (0.228 g, 73% yield) as pale brown solid. Mp–273–275 °C. <sup>1</sup>H NMR (DMSO-*d*<sub>6</sub>): δ<sub>H</sub> 4.21 (s, 4H), 7.03–8.26 (m, 7H) 10.16 (s, 1H), 12.61 (b, 1H). <sup>13</sup>C NMR (DMSO-*d*<sub>6</sub>): δ<sub>C</sub> 173.4, 169.8, 162.2, 150.7, 145.6, 138.8, 130.8, 128.9, 123.8, 122.6, 120.3, 70.2, 67.8. EI-MS  $m/z$ : 327.4 (M+H)<sup>+</sup>. Anal. Calcd for C<sub>16</sub>H<sub>14</sub>N<sub>4</sub>O<sub>4</sub>: C, 58.89; H, 4.32; N, 17.17. Found: C, 58.91; H, 4.30; N, 17.19.

**4.2.11.12. 2-(2-((4-(3H-Imidazo[4,5-*b*]pyridin-2-yl)phenyl)amino)-2-oxoethyl)thio)acetic acid (44).** The compound was prepared according to the general procedure D using 4-(3H-imidazo[4,5-*b*]pyridin-2-yl)aniline **3f** (0.1 g, 0.48 mmol), triethylamine, acid (0.12 g, 1.2 mmol), 2,2'-thiodiacetic acid (0.071 g, 0.48 mmol) and propylphosphonic anhydride solution (0.38 g, 1.2 mmol) to afford **44** (0.232 g, 71% yield) as brown solid. Mp–250–252 °C. <sup>1</sup>H NMR (DMSO-*d*<sub>6</sub>): δ<sub>H</sub> 3.26 (s, 2H), 3.39 (s, 2H), 7.02–8.27 (m, 7H) 10.14 (s, 1H), 12.73 (b, 1H). <sup>13</sup>C NMR (DMSO-*d*<sub>6</sub>): δ<sub>C</sub> 174.8, 168.5, 161.8, 150.6, 145.3, 138.8, 130.8, 128.5, 123.8, 122.6, 120.2, 43.8, 41.5. EI-MS  $m/z$ : 343.5 (M+H)<sup>+</sup>. Anal. Calcd for C<sub>16</sub>H<sub>14</sub>N<sub>4</sub>O<sub>3</sub>S: C, 56.13; H, 4.12; N, 16.36. Found: C, 56.16; H, 4.09; N, 16.38.

### 4.3. Biological activity

#### 4.3.1. *E. coli* DNA gyraseA and *S. aureus* DNA gyraseB cloning, protein expression and purification

While the vectors were from Qiagen, the primers from Sigma–Aldrich and all the enzymes unless otherwise mentioned

were from New England Biolabs. *E. coli* DNA gyraseA gene was amplified using a forward primer 5' CACCCATATGCTACGTTATGGTTACCGC 3' and a reverse primer 5' AGCTGCGGCCGCCACTGCCAGCA TATTGCA 3' from the genomic DNA of *E. coli* DH5α strain. Subsequently, the amplified PCR products were further digested with NdeI and NotI and cloned into NdeI and NotI sites of pQE2 vector under T5 promoter with His tag at N-terminal domain in our laboratory. Similarly, the gene encoding *S. aureus* DNA gyraseB was amplified from *S. aureus* RN4220 genomic DNA by using the forward primer 5' CACCCATATGGTGACTGCATTGTCAGA 3' and a reverse primer 5' AGCTAAGCTTTAGAAAGTCTAAGTTTGCAT 3' flanked with NdeI and HindIII sites. These digested products were ligated at the same site of the pQE2 vector, downstream of the T5 promoter with an N-terminal His tag, the clones were later authenticated by sequencing using a sequencer. Final clones were confirmed by sequencing in a sequencer. Further, for expression of these clones, they were transformed into BL21-codon plus (DE3) cells of *E. coli*. Transformants were grown in Luria Bertani (LB) broth (Himedia) at 37 °C with shaking (rpm 140), in the presence of ampicillin (100 µg/mL) (Sigma) until the starting optical density of 0.1 reached the value of 0.4–0.6. The protein expression was induced with 0.2 mM IPTG (Himedia) and further grown overnight for induction of the protein, at 18 °C. Cells were harvested by centrifugation (5500 rpm, 4 °C, 15 min) and suspended in lysis buffer containing 20 mM Tris–HCl (pH 7.4), 0.1 M NaCl, 2 mM KCl, 10 mM Na<sub>2</sub>HPO<sub>4</sub>, 1.3 mM K<sub>2</sub>HPO<sub>4</sub>, 5% Glycerol, 1 mM DTT, 1:200 µL protease inhibitor cocktail. The mixture was further sonicated (amplitude 35%, 1 s on 2 s off for 4 min) and was centrifuged (12,000 rpm, 4 °C 20 min). To the supernatant, pre-equilibrated Ni-NTA beads (GE Healthcare) were mixed and swirled for 1 h in cold room, centrifuged at 500 rpm for 5 min at 4 °C, the pellets were redissolved in lysis buffer and loaded onto the Bio-Rad column, each loaded fraction was washed with 50 mL Tris–HCl (pH 7.4), 500 mM NaCl, 2 mM KCl, 10 mM Na<sub>2</sub>HPO<sub>4</sub>, 1.3 mM K<sub>2</sub>HPO<sub>4</sub>, 5% Glycerol, 1 mM DTT. Protein was eluted with 25 mM Tris–HCl (pH 8), 140 mM NaCl, 5% Glycerol, 1 mM DTT, and 1 mM PMSF. Initial wash was done with elution buffer without imidazole (Himedia). Subsequently, various imidazole concentration gradients were included from 5 mM to 500 mM. Samples were collected in autoclaved 2 mL eppendorf tubes. Dialysis was performed 4 times overnight against (25 mM Tris–HCl pH 7.4, 140 mM NaCl, 15% glycerol, 2 mM dithiothreitol, 1 mM EDTA), and dialyzed protein was concentrated at (3000 rpm, 4 °C) to a final concentration of 2.5 mg/mL. Later the purity of the protein was analysed by SDS PAGE method. A 20 µL volume of the dialyzed protein was applied on the polyacrylamide gel (1 mm, 10%), and 5 µL of a commercially available protein molecular weight marker (Bio-Rad) was added. The electrophoresis was run in 1X TBE buffer (Tris–HCl pH 7.5, 1 mM boric acid, 1 mM EDTA) for a period of 90 min at a constant voltage. Later the gel was transferred to a solution of Coomassie Brilliant Blue dye mixed with 20% acetic acid. After 20 min of shaking in an orbital shaker, it was destained several times with 10% acetic acid in 30% methanol and 60% of water until the complete staining is lost and transparency of the gel was achieved. Subsequently, the purity of the protein was determined to be >90% as only single bands corresponding to its molecular weight of *S. aureus* gyraseB was observed between 70 and 80 kDa, while that of *E. coli* gyraseA was observed between 90 and 99 kDa.

#### 4.3.2. In vitro screening of the compounds for inhibitory activity and determination of IC<sub>50</sub> values through ATPase assay

The proteins were expressed as described in Section 4.3.1. As reported earlier, the purified *S. aureus* gyraseB does not have a highly active ATPase activity like *E. coli* gyraseB.<sup>22</sup> Hence gyraseB assay was performed with recombinant proteins of *E. coli* gyraseA and *S. aureus* gyraseB.<sup>19,23</sup> As per the reports, the reaction is

activated to about 620 fold with incorporation of small molecular weight DNA, in the assay as it is reported to stimulate the protein.<sup>23</sup> Initially, equimolar quantities of about 0.5  $\mu\text{M}$  each of *E. coli* gyraseA and *S. aureus* gyraseB were incubated for a period of 45 min with salmon sperm DNA (Sigma) in 50 mM Tris (pH 7.5), 75 mM ammonium acetate buffer for the reconstitution of the hybrid topoisomerases at 4 °C. Later the assay was performed in a 96-well microtiter plate as mentioned earlier.<sup>37</sup> The assay buffer includes 50 mM Tris (pH 7.5), 75 mM ammonium acetate, 5% w/v glycerol, 0.5 mM EDTA, 6 mM magnesium chloride, 0.001% Triton X-100, 1 mM dithiothreitol, DNA of 2  $\mu\text{g}/\text{mL}$  ( $\sim 3$   $\mu\text{M}$  base pairs), 250  $\mu\text{M}$  ATP, 2.2 nM of *E. coli* gyraseA and *S. aureus* gyraseB. Reactions were performed with various drug concentration ranges for the calculation of  $\text{IC}_{50}$ , with a negative moxifloxacin and positive novobiocin control as standards. The reaction was allowed to proceed for 60 min and was quenched by addition of 20  $\mu\text{L}$  of malachite green reagent (POMG-25H, Bioassay systems, USA) subsequently absorbance was read at 650 nm after 20 min incubation. Triton X-100 acts as a surfactant to prevent aggregation of molecules during the assay.

#### 4.3.3. Determination of *S. aureus* DNA gyrase supercoiling activity<sup>38</sup> with ( $\text{IC}_{50}$ ) determination

Supercoiling assay was performed using the commercially available kit (DNA gyrase supercoiling assay kit: SAS4001) from Inspiralis Pvt. limited, Norwich, UK. The assay was performed in 1.5 mL eppendorf tubes at room temperature. 1 U of *S. aureus* DNA gyrase was incubated with 0.5  $\mu\text{g}$  of relaxed pBR 322 DNA in 30  $\mu\text{L}$  reaction volume at 37 °C for 30 min with 40 mM HEPES, KOH (pH 7.6), 10 mM magnesium acetate, 10 mM DTT, 2 mM ATP, 500 mM potassium glutamate, 0.05 mg/mL albumin (BSA). Standard compound novobiocin was the positive control and 4% DMSO was considered as negative control. Subsequently, each reaction was stopped by the addition of 30  $\mu\text{L}$  of Stop dye [40% sucrose, 100 mM Tris–HCl (pH 7.5), 1 mM EDTA and 0.5 mg/mL bromophenol blue],<sup>39</sup> briefly centrifuged for 45 s and was run in 1% agarose gel in 1X TAE buffer (40 mM Tris acetate, 2 mM EDTA). Furthermore, concentration of the range of compounds that inhibits 50% of supercoiling activity ( $\text{IC}_{50}$ ) was determined using densitometry and NIH image through Bio-Rad GelDoc image viewer.

#### 4.3.4. Antimicrobial activity measurements

The *Staphylococcus aureus* bacterial culture (MTCC 3160) was obtained from Microbial Type Culture Collection and Gene Bank, Chandigarh, India while the MRSA 96 strain was obtained from Sir Ronald Ross Institute of Tropical and Communicable Diseases (Nallakunta, India). Minimum inhibitory concentrations for the test compounds were determined by agar dilution method<sup>40</sup> according to Clinical and Laboratory Standards Institute guidelines.<sup>41</sup> The antibacterial activity study for forty one compounds was performed at the Department of Pharmacy, Birla Institute of Technology and Science, Hyderabad on both the strains separately. Fresh overnight colonies from Mueller–Hinton agar (Hi-Media) medium were suspended to a turbidity of approximately  $10^6$  colony forming units (cfu)/mL. Stock solutions of tested compounds and standards (ciprofloxacin and ofloxacin) were prepared in 0.9% saline. A control was set for the comparison of the test compounds. A total of 1 mL of the bacterial suspension was added to plates containing 19 mL of the media, so the test range was about 10 doubling dilutions from 100  $\mu\text{M}$  to 0.1  $\mu\text{M}$ . The plates were incubated at 35 °C in ambient air for about 16–20 h. The minimum inhibitory concentration (MIC) for the compounds was considered to be the lowest drug concentration that prevented the visible growth of the bacteria on the agar plates.

#### 4.3.5. Inhibitions of biofilm formation

Biofilm assay was carried out in 96-well tissue culture plate (TCP) method as described by Christensen et al.<sup>42</sup> Detection of the biofilm formation by the MRSA 96 strain was done as reported earlier by the Congo red agar media (CRA)<sup>43</sup> method. Though certain disadvantages are associated with this method, yet it was followed due to its simple, economic and efficient process.<sup>43</sup> The screening was done using specially prepared solid medium that is brain heart infusion broth (BHI) (Himedia) supplemented with 5% sucrose. Congo red stain was prepared as concentrated solution and autoclaved at 121 °C for 15 min, added when the agar had cooled to 55 °C.<sup>43</sup> The strain was inoculated on to the plates prepared, incubated for 36 h at 37 °C aerobically. The observation of the black colonies has confirmed the biofilm producing nature of the MRSA strain. Subsequently, the assay was performed in a 96-well flat bottom tissue culture plate in trypticase soy broth with 1% glucose (TSB) (Himedia).

##### 4.3.5.1. Quantitative assay of the biofilm formed on 96-well microtiter plates.

Isolates from agar plate were inoculated in TSB media and incubated for 18 h at 37 °C with 120 rpm. Later the culture was diluted 1 in 100 with fresh TSB medium and 200  $\mu\text{L}$  of it was aliquoted into each of the wells along with the test compounds at different concentrations of 100–1.56  $\mu\text{M}$ , while the control was incubated with DMSO solvent, though the DMSO usage was limited to 4% during the assay. The plates were incubated for 24 h at 37 °C in stationary phase with the lid closed. The contents of each well was gently removed by tapping the plates inverted, the plates were washed thrice with 0.2 mL of phosphate buffer saline (PBS) at pH 7.2 to remove the unattached, dead and free floating planktonic bacteria. The biofilm formed by adherent sessile *S. aureus* MRSA 96 was fixed with sodium acetate (2%) and stained with (0.1%w/v) crystal violet. As the crystal violet stains the dead and live cells, it is limited to certain use, but in this assay the wells were washed thrice so the chance of unattached dead cells staining is almost neglected.<sup>43</sup> Excess stain was rinsed off by thorough washing with water and plates were dried in a hot air oven. The plates were photographed. For the quantitative estimation, absorbance was read at 570 nm by Perkin Elmer Victor X3 plate reader. The optical density (OD) values reflected an index of the *S. aureus* bacteria adhering to surface and forming biofilm. The experiment was performed in triplicates, the background absorbance was compensated by reading the OD from sterile medium, fixative used, auto absorbance and dye which were averaged and subtracted from all test values, and this mean OD was also subtracted from the control well too. The control well OD was 0.28 which indicated that the MRSA 96 strain was a strong biofilm producer. In general, OD values above 0.2 are considered as strong biofilm producers.<sup>44</sup> The inhibition percentage of the tested compounds was calculated by the formula.

$$\% \text{ Inhibition} = \frac{\text{control reading} - \text{blank reading}}{\text{control reading}} * 100.$$

Further, the dry crystal violet stained plates were treated with 200  $\mu\text{L}$  of 33% glacial acetic acid, given a brief shake in orbital shaker and the plates were read at 570 nm in a Perkin Elmer Victor X3 96-well plate reader. The OD gives us the approximate count of the cells involved in the biofilm formation.

#### 4.3.6. Mammalian cytotoxicity studies

A diploid human embryonic kidney cell line (HEK-293) from ATCC was used to assess the cytotoxicity of all the forty one test compounds as described before.<sup>45</sup> Briefly, HEK-293 cells were seeded at 5000 cells per well in a 96-well microtiter plate (NEST). After 24 h incubation, the cells were washed with PBS and 2-fold

dilutions of the drug was made in 200  $\mu$ L of standard culture medium (RPMI + 5% FBS + 1% penicillin and streptomycin) were added, while the final DMSO concentration of the culture was limited to 0.5%. Further, the cultures were incubated with a drug concentration of 100  $\mu$ M at 37 °C in 5% CO<sub>2</sub>/95% air for 72 h. Untreated cultures with DMSO were included as controls. The viability of the cells was assessed on the basis of cellular conversion of the dye MTT (Methylthiazol-tetrazolium) into formazan crystals using Perkin Elmer Victor X3 Titre 96 plate reader at 570 nm. Ciprofloxacin (3% inhibition) and novobiocin (9.8% inhibition) were used as positive controls.

#### 4.3.7. In vivo efficacy in mouse septicemia model

The in vivo antibacterial activity of the test compounds was determined in CD-1 female mice (20–25 g bodyweight, ten per group). The mice were infected intraperitoneally with a suspension containing an amount of the indicated organism slightly greater than its lethal dose 100 ( $3 \times 10^7$  cfu/mouse). The mice were treated orally intravenous (iv) with a specific amount of the test compound administered after 4 h infection. Survival was assessed 24 h post infection.

#### 4.3.8. hERG (orthologous to human ether-a-go-go-related gene) channel inhibition studies

hERG studies were conducted using zebrafish larval model. Zebrafish were procured commercially from Vikrant Aquaculture, Mumbai, India. They were maintained in a recirculatory system containing 0.06% sea salt under 14 h light and 10 h dark cycle and 28 °C water temperature.<sup>46</sup> Males and females were maintained in different tanks before they were allowed to breed. Breeding of zebrafish were allowed in the ratio of 2 females: 3 males under the sudden stimulation of light. Subsequently, embryos were collected into petridish containing E3 medium (5 mM NaCl, 0.17 mM KCl, 0.33 mM CaCl<sub>2</sub> and 0.33 mM MgSO<sub>4</sub>) and incubated at 28 °C temperature.<sup>47</sup> In this assay 3 dpf embryos were distributed in a 24-well plate along with 250  $\mu$ L of 0.1% DMSO solution, while the stocks were prepared in 100% DMSO, working concentrations of the compound was prepared by serial dilutions. Each well containing 5 embryos were treated with each required concentration of the solution and incubated at 28 °C for 4 h. Later, individual embryo of each well was focused under light microscope (Leica) and heartbeat was observed (i.e., atrial and ventricular beats). The time taken for 30 beats was measured with the help of stopwatch while the mean for the time taken by 5 embryos was calculated for each well. Subsequently, the number of heart beats per minute was calculated as follows:

$$1800/X = \text{beats/minute (where } X = \text{time in seconds)}$$

#### 4.3.9. Differential scanning fluorimetry (DSF): biophysical and structural evaluation of benzimidazole chemical class

The active compounds from this series of chemical class of molecules were further investigated using a biophysical technique, differential scanning fluorimetry. The ability of the compounds to stabilize the catalytic domain of the gyrase protein was assessed utilizing the DSF technique by which the thermal stability of the catalytic domain of gyraseB native protein and of the protein with the ligand is measured.<sup>7</sup> Complex with compound **10** were heated stepwise from 25 °C to 95 °C in steps of 0.6 °C in the presence of the fluorescent dye, whose fluorescence increases as it interacts with hydrophobic residues of the gyraseB protein. As the protein gets denatured the amino acid residues become exposed to the dye.<sup>9</sup> A right side positive shift of  $T_m$  in comparison to native protein means higher stabilization of the protein-ligand complexes, which is a consequence of the inhibitor binding.<sup>36</sup>

#### Acknowledgments

We are sincerely grateful to Prof. M. Meera and Gujjula Ravi Kumar (Sir Ronald Ross Institute of Tropical and Communicable Diseases (Nallakunta, India), Osmania University for help with *S. aureus* MRSA 96 strain.

#### Supplementary data

Supplementary data (additional experimental details concerning e-pharmacophore modelling, docking studies, QikProp results) associated with this article can be found, in the online version, at <http://dx.doi.org/10.1016/j.bmc.2014.09.008>.

#### References and notes

- McAdam, P. R.; Templeton, K. E.; Edwards, G. F.; Holden, M. T.; Feil, E. J.; Aanensen, D. M.; Bargawi, H. J.; Spratt, B. G.; Bentley, S. D.; Parkhill Proc. Natl. Acad. Sci. **2012**, *109*, 9107.
- Lele, A. C.; Tawari, N. R.; Degani, M. S. *Int. J. Pharm. Biosci. Technol.* **2013**, *1*, 34.
- Ginzburg, E.; Namias, N.; Brown, M.; Ball, S.; Hameed, S. M.; Cohn, S. M. *Int. J. Antimicrob. Agents* **2000**, *16*, 39.
- Eakin, A. E.; Green, O.; Hales, N.; Walkup, G. K.; Bist, S.; Singh, A.; Mullen, G.; Bryant, J.; Embrey, K.; Gao, N. *Antimicrob. Agents Chemother.* **2012**, *56*, 1240.
- Waters, E. M.; Rudkin, J. K.; Schaeffer, C. R.; Lohan, A. J.; Tong, P.; Loftus, B. J.; Fey, P. D.; Massey, R. C.; O'Gara, J. P.; Pozzi, C. *PLoS Pathog.* **2012**, *8*, 1002626.
- Basarab, G. S.; Manchester, J. I.; Bist, S.; Dangel, B.; Illingworth, R.; Sriram, S.; Boriack-Sjodin, P. A.; Sherer, B. A.; Uria-Nickelsen, M.; Eakin, A. J. *Med. Chem.* **2013**, *56*, 8712.
- Brvar, M.; Perdih, A.; Renko, M.; Anderluh, G.; Turk, D. A.; Solmajer, T. *J. Med. Chem.* **2012**, *55*, 6413.
- Maxwell, A. *Trends Microbiol.* **1997**, *5*, 102.
- Brvar, M.; Perdih, A.; Hodnik, V.; Renko, M.; Anderluh, G.; Jerala, R.; Solmajer, T. *Bioorg. Med. Chem.* **2012**, *20*, 2572.
- Champoux, J. *J. Annu. Rev. Biochem.* **2001**, *70*, 369.
- Minovski, N.; Perdih, A.; Solmajer, T. *J. Mol. Model.* **2012**, *18*, 1735.
- Fournier, B.; Zhao, X.; Lu, T.; Drlica, K.; Hooper, D. C. *Antimicrob. Agents Chemother.* **2000**, *44*, 2160.
- Jackson, A. P.; Maxwell, A. *Proc. Natl. Acad. Sci.* **1993**, *90*, 11232.
- Garry, M. W. *The Am. J. Med. Sci.* **1958**, *236*, 330.
- Oblak, M.; Kotnik, M.; Solmajer, T. *Curr. Med. Chem.* **2007**, *14*, 2033.
- Lafitte, D.; Lamour, V.; Tsvetkov, P. O.; Makarov, A. A.; Klich, M.; Deprez, P.; Moras, D.; Briand, C.; Gilli, R. *Biochemistry* **2002**, *41*, 7217.
- Angehern, P.; Goetschi, E.; Gmuender, H.; Hebeisen, P.; Hennig, M.; Kuhn, B.; Luebbbers, T.; Reindl, P.; Ricklin, F.; Schmitt-Hoffmann, A. *J. Med. Chem.* **2011**, *54*, 2207.
- Ronkin, S. M.; Badia, M.; Bellon, S.; Grillot, A.-L.; Gross, C. H.; Grossman, T. H.; Mani, N.; Parsons, J. D.; Stamos, D.; Trudeau, M. *Bioorg. Med. Chem. Lett.* **2010**, *20*, 2828.
- Sherer, B. A.; Hull, K.; Green, O.; Basarab, G.; Hauck, S.; Hill, P.; Loch, J. T., III; Mullen, G.; Bist, S.; Bryant, J. *Bioorg. Med. Chem. Lett.* **2011**, *21*, 7416.
- Friesner, R. A.; Murphy, R. B.; Repasky, M. P.; Frye, L. L.; Greenwood, J. R.; Halgren, T. A.; Sanschagrin, P. C.; Mainz, D. T. *J. Med. Chem.* **2006**, *49*, 6177.
- Poyraz, O. M.; Jeankumar, V. U.; Saxena, S.; Schnell, R.; Haraldsson, M.; Yogeewari, P.; Sriram, D.; Schneider, G. *J. Med. Chem.* **2013**, *56*, 6457.
- Blanche, F.; Cameron, B.; Bernard, F.-X.; Maton, L.; Manse, B.; Ferrero, L.; Ratet, N.; Lecoq, C.; Goniot, A.; Bisch, D. *Antimicrob. Agents Chemother.* **1996**, *40*, 2714.
- Eakin, A.; Ehmann, D.; Gao, N.; Karantzeni, I.; Walkup, G.; Google Patents. **2004**.
- Ince, D.; Zhang, X.; Hooper, D. C. *Antimicrob. Agents Chemother.* **2003**, *47*, 1410.
- Donlan, R. M. *J. Clin. Infect. Dis.* **2001**, *33*, 1387.
- (a) Donlan, R. M. *Emerg. Infect. Dis.* **2001**, *7*, 277; (b) Barie, P. S. *World J. Surg.* **1998**, *22*, 118.
- Smith, K.; Perez, A.; Ramage, G.; Lappin, D.; Gemmell, C. G.; Lang, S. *J. Med. Microbiol.* **2008**, *1018*, 57.
- Giacometti, A.; Cirioni, O.; Gov, Y.; Ghiselli, R.; Del Prete, M. S.; Mucchegiani, F.; Saba, V.; Orlando, F.; Scalise, G.; Balaban, N. *Antimicrob. Agents Chemother.* **1979**, *2003*, 47.
- Ma, Y.; Xu, Y.; Yestrepky, B. D.; Sorenson, R. J.; Chen, M.; Larsen, S. D.; Sun, H. *PLoS ONE* **2012**, *7*, 47255.
- Sriram, D.; Yogeewari, P.; Basha, J. S.; Radha, D. R.; Nagaraja, V. *Bioorg. Med. Chem.* **2005**, *13*, 5774.
- Alexandrou, A. J.; Duncan, R. S.; Sullivan, A.; Hancox, J. C.; Leishman, D. J.; Witche, H. J.; Leaney, J. L. *Br. J. Pharmacol.* **2006**, *147*, 905.
- Chen, X.; Cass, J. D.; Bradley, J. A.; Dahm, C. M.; Sun, Z.; Kadoszewski, E.; Engwall, M. J.; Zhou, J. *Br. J. Pharmacol.* **2005**, *146*, 792.
- Ahuja, V.; Sharma, S. *J. Appl. Toxicol.* **2013**, *34*, 576.
- Milan, D. J.; Peterson, T. A.; Ruskin, J. N.; Peterson, R. T.; MacRae, C. A. *Circulation* **2003**, *107*, 1355.
- Mittelstadt, S.; Hemenway, C.; Craig, M.; Hove, J. *J. Pharmacol. Toxicol. Methods* **2008**, *57*, 100.
- Niesen, F. H.; Berglund, H.; Vedadi, M. *Nat. Protoc.* **2007**, *2*, 2212.

37. Green, O. M.; Hull, K. G.; Ni, H.; Hauck, S. I.; Mullen, G. B.; Breeze, A. L.; Hales, N. J.; Timms, D.; Google Patents. 2010.
38. Hossion, A. M.; Zamami, Y.; Kandahary, R. K.; Tsuchiya, T.; Ogawa, W.; Iwado, A.; Sasaki, K. *J. Med. Chem.* **2011**, *54*, 3686.
39. Hallett, P.; Grimshaw, A.; Wigley, D.; Maxwell, A. *Gene* **1990**, *93*, 139.
40. Pandeya, S.; Sriram, D.; Nath, G.; DeClercq, E. *Eur. J. Pharmacol. Sci.* **1999**, *9*, 25.
41. Ferraro, M. J.; NCCLS: 2000.
42. Christensen, G. D.; Simpson, W.; Younger, J.; Baddour, L.; Barrett, F.; Melton, D.; Beachey, E. *J. Clin. Microbiol.* **1985**, *22*, 996.
43. Freeman, D.; Falkiner, F.; Keane, C. *J. Clin. Pathol.* **1989**, *42*, 872.
44. Mathur, T.; Singhal, S.; Khan, S.; Upadhyay, D.; Fatma, T.; Rattan, A. *Indian J. Med. Microbiol.* **2006**, *24*, 25.
45. Sriram, D.; Senthilkumar, P.; Dinakaran, M.; Yogeewari, P.; China, A.; Nagaraja, V. *J. Med. Chem.* **2007**, *50*, 6232.
46. Banote, R. K.; Koutarapu, S.; Chennubhotla, K. S.; Chatti, K.; Kulkarni, P. *Epilepsy Behav.* **2013**, *27*, 212.
47. Jung, T.-P.; Makeig, S.; Westerfield, M.; Townsend, J.; Courchesne, E.; Sejnowski, T. J. *Clin. Neurophysiol.* **2000**, *111*, 1745.